IEEE TRANSACTIONS ON

SIGNAL PROCESSING

A PUBLICATION OF THE IEEE SIGNAL PROCESSING SOCIETY

IEEE Signal Processing Society

www.signalprocessingsociety.org

Indexed in PubMed® and MEDLINE®, products of the United States National Library of Medicine

PubMed MEDLINE U.S. National Library of Medicine

JULY 2011 VOLUME 59 NUMBER 7 ITPRED (ISSN 1053-587X)

REGULAR PAPERS

(Contents Continued on Back Cover)

IEEE

(Contents Continued from Front Cover)

Computationally Efficient Subspace-Based Method for Two-Dimensional Direction Estimation With L-Shaped Array

Guangmin Wang, *Student Member, IEEE*, Jingmin Xin, *Senior Member, IEEE*, Nanning Zheng, *Fellow, IEEE*, and Akira Sano, *Member, IEEE*

***Abstract*—In order to mitigate the effect of additive noises and reduce the computational burden, we propose a new computationally efficient cross-correlation based two-dimensional (2-D) direction-of-arrivals (DOAs) estimation (CODE) method for noncoherent narrowband signals impinging on the L-shaped sensor array structured by two uniform linear arrays (ULAs). By estimating the azimuth and elevation angles independently with a one-dimensional (1-D) subspace-based estimation technique without eigendecomposition, where the null spaces are obtained through a linear operation of the matrices formed from the cross-correlation matrix between the received data of two ULAs, then the pair-matching of estimated azimuth and elevation angles is accomplished by searching the minimums of a cost function of the azimuth and elevation angles, where the computationally intensive and time-consuming eigendecomposition process is avoided. Further the asymptotic mean-square-error (MSE) expressions of the azimuth and elevation estimates are derived. The effectiveness of proposed method and the theoretical analysis are verified through numerical examples, and it is shown that the proposed CODE method performs well at low signal-to-noise ratio (SNR) and with a small number of snapshots.**

***Index Terms*—Direction-of-arrival (DOA) estimation, eigendecomposition, pair-matching, uniform linear array (ULA).**

I. Introduction

TWO-DIMENSIONAL (2-D) direction-of-arrivals (DOAs) (i.e., elevation and azimuth angles) estimation of multiple signals by using planar arrays with various array geometries plays an important role in many practical applications such as sonar, radar, and communications, and it has been well studied in the literature (see, e.g., [12]–[27], and references therein). Due to the increase in the dimensionality of the 2-D DOA estimation problem, the computational complexity of DOA estimation process is severely affected by the array geometry [14], [15], and further the pair-matching (i.e., association or alignment) of the estimated elevation and azimuth angles is usually required [13], [14], [23]–[27], where most conventional pairing algorithms involve 2-D searching and/or nonlinear optimization. Hence much efforts have focused on reducing the computational complexity of the 2-D estimation problem and facilitating the estimation algorithm.

In recent years, some planar sensor arrays formed with two or more uniform linear arrays (ULAs) with simple and specified geometry configurations have received considerable attention (e.g., [1]–[7], [28]–[31]), where the 2-D DOAs of multiple incident signals can be estimated with reduced computational complexity by applying most one-dimensional (1-D) subspace-based estimation methods such as the ESPRIT (estimation of signal parameters via rational invariance techniques) method [32] and its variants [33], [34], which have been extensively studied in the literature (cf. [10], [12] and references therein), whereas the crux is the pair-matching of the elevation and azimuth angles estimated separately. Especially the L-shaped array composed of two ULAs connected orthogonally at the one end of each ULA (i.e., shifted cross array) has some advantages in coverage area and implementation [1], [3], [4], and several DOA estimation methods were developed for narrowband signals impinging on the L-shaped array placed in the $x-y$ plane [1], [18], [23]. By exploiting the geometric structure of the L-shaped array, a relatively efficient maximum likelihood (ML) method was proposed for DOA estimation [1], where the orthogonality of signal and noise subspaces based pairing technique was also given, but good initial estimates are required to make the iterative ML algorithm converge to the global optimum point. By employing the shift invariance and conjugate centrosymmetry of the ULA, a closed-form unitary ESPRIT method was applied to the L-shaped array with automatic pairing by using real-valued eigendecomposition either in element space or beamspace [18]. Additionally a matrix pencil based noniterative method was suggested to estimate the directions independently from the received data of each array [23], where two estimates of polarization ratio were used to search all the possible pairs of the estimated elevation and azimuth angles, and the partition and stacking of the received data matrix increase the computational burden of the involved eigendecomposition process.

Manuscript received September 18, 2010; revised January 22, 2011; accepted April 04, 2011. Date of publication April 21, 2011; date of current version June 15, 2011. The associate editor coordinating the review of this manuscript and approving it for publication was Prof. Shahram Shahbazpanahi. This work was supported in part by the National Natural Science Foundation of China by Grant 60772096 and by the State Key Development Program for Basic Research of China under Grants 2007CB311005 and 2010CB327902. This work was presented at the IEEE 11th Signal Processing Workshop on Signal Processing Advances in Wireless Communications (SPAWC'10), Marrakech, Morocco, June 2010.

G. Wang and N. Zheng are with the Institute of Artificial Intelligence and Robotics, Xi'an Jiaotong University, Xi'an 710049, China (e-mail: gm.wang@stu.xjtu.edu.cn; nnzheng@mail.xjtu.edu.cn).

J. Xin is with the Institute of Artificial Intelligence and Robotics, Xi'an Jiaotong University, Xi'an 710049, China, and he is also with Xi'an Jiaotong University Suzhou Academy, Suzhou 215123, China (e-mail: jxin@mail.xjtu.edu.cn)

A. Sano is with the Department of System Design Engineering, Keio University, Yokohama 223-8522, Japan (e-mail: sano@sd.keio.ac.jp).

Digital Object Identifier 10.1109/TSP.2011.2144591

On the other hand, more recently some new direction estimation methods were proposed for the L-shaped array placed in the $x-z$ plane in attempt to solve the 2-D estimation problem in more computationally efficient way [3]–[5], [7], [31]. By utilizing the shift invariance and the partition of array response vector of two overlapping subarrays of each ULA, a modified propagator method (MPM) with eigendecomposition was presented to estimate the elevation and azimuth angles independently from the covariance matrix of combined received data of two overlapping subarrays of each ULA [3]. However unlike the ordinary propagator method (PM) [9], the least-square (LS) estimation of the linear propagator is seriously affected by the nonzero correlations of additive noises between two overlapping subarrays, and correspondingly the angle estimates are biased regardless of the signal-to-noise ratio (SNR). Furthermore a pair-matching procedure is still required to associate the elevation and azimuth estimates due to the independent orderings of the array response vectors of two ULAs in terms of the elevation or azimuth angles and that of eigenvalues of two above-mentioned covariance matrices for 1-D DOA estimation with respect to each ULA [4], [8]. By dividing one ULA into two overlapping subarrays to gain the shift invariance of these subarrays, a joint singular value decomposition (SVD) based method (JSVD) was suggested to 2-D DOA estimation with automatic pairing by using two cross-correlation matrices (CCMs) between two subarrays and another ULA [5], where the effect of additive noise is mitigated. The key point of [5] and its variants [35], [36] is the ordering exchange of a product of the source signal covariance matrix and a diagonal matrix of the phase delays with respect to the elevation or azimuth angle, which is only valid when the source signal covariance matrix is diagonal matrix. Unfortunately the JSVD [5] performs worse in the estimation of azimuth angle even in the case of uncorrelated signals when the number of snapshots is small, because the nonzero cross-correlations in the estimated source signal covariance matrix couple up the array response vectors in terms of the azimuth angle, and it results in inaccurate parameter estimate even at high SNR. An alternative cross-correlation matrix and SVD based method was proposed for 2-D DOA estimation with automatic pairing [7], but it involves the minimization of a constrained nonlinear function and necessitates *a prior* knowledge of the powers of incident signals. By introducing an auxiliary electrical angle as a function of the elevation and azimuth angles and adopting the 1-D generalized ESPRIT method [34], a joint estimation method was proposed without pair-matching procedure [31], however it requires two computationally intensive eigenvalue decomposition (EVD) processes and a restriction on the elevation and azimuth angles. In addition, an elaborative CCM based pair-matching method was developed [4], but it is seriously affected by the estimation of the "virtual angles" of incident signals even though the elevation and azimuth angles are estimated well [5].

Therefore the purpose of this paper is to investigate the 2-D DOA estimation of noncoherent narrowband signals with the L-shaped array placed in the $x-z$ plane in a new computationally efficient way. Since the eigendecomposition (EVD or SVD) process is computationally intensive and time-consuming [37], some computationally simple subspace-based 1-D DOA estimation methods were proposed without eigendecomposition (see [10] and references therein). In order to alleviate the effect of additive noise and to reduce the computational burden involved by eigendecomposition, we proposed a subspace-based method without eigendecomposition (SUMWE) for 1-D DOA estimation with the ULA [10], where the full ULA is divided into overlapping forward and backward subarrays, and the null space is obtained through a linear operation of the combined Hankel correlation matrix, which is formed from the cross-correlations of some sensor data by exploiting the shift invariance of ULA, where the effect of additive noise is mitigated. Inspired by the SUMWE, we propose a new computationally efficient cross-correlation based 2-D DOA estimation (CODE) method without eigendecomposition by exploiting the array geometry of L-shaped array. Firstly the elevation and azimuth angles are estimated independently by a 1-D subspace-based estimation technique, where the null spaces are obtained through a linear operation of the matrices formed from the cross-correlation matrix between the array data received by two ULAs, and then the pair-matching can be conducted by searching the minimums of a cost function of the azimuth and elevation angles, where the eigendecomposition is avoided in the both procedures. Moreover the statistical analysis of the proposed DOA estimation method is studied, and the explicit expressions of the asymptotic mean-square-errors (MSEs) of the elevation and azimuth estimates are derived. The effectiveness of proposed method and the theoretical analysis are substantiated through numerical examples. The simulation results show that the proposed CODE method has good estimation with a small number of snapshots and at low SNR and there is good agreement between the theoretical analyzes and empirical results.

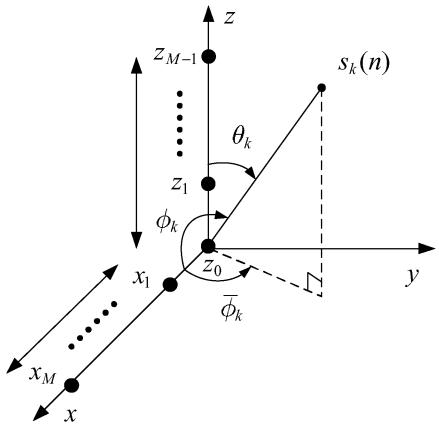

Fig. 1. The geometrical configuration of the L-shaped array for 2-D direction estimation [4].

II. Data Model and Assumptions

As shown in Fig. 1, we consider the L-shaped array consisting of two ULAs in the $x-z$ plane, where each ULA has M omnidirectional sensors with spacing d, the sensor at the origin of coordinates z_0 is the reference one for each ULA, and the interelement spacing between the sensors z_0 and x_1 of these ULAs is also d, and we suppose that p noncoherent narrowband signals

$\{s_k(n)\}$ with the wavelength λ are in the far-field and imping on the array from distinct directions with the elevation and azimuth angles $\{\theta_k, \phi_k\}$ [1], [4], where the elevation angle θ_k and the azimuth angle ϕ_k are measured clockwise relatively to the z or x axis, while the projected azimuth angle $\bar{\phi}_k$ is measured counterclockwise relatively to the x axis in the $x-y$ plane. Then the received signals at the ULAs along the z and x axes are given by

$$\boldsymbol{z}(n) = \boldsymbol{A}(\theta)\boldsymbol{s}(n) + \boldsymbol{w}_z(n) \tag{1}$$

$$\boldsymbol{x}(n) = \boldsymbol{A}(\phi)\boldsymbol{s}(n) + \boldsymbol{w}_x(n) \tag{2}$$

where $\boldsymbol{z}(n) \triangleq [z_0(n), z_1(n), \cdots, z_{M-1}(n)]^T$, $\boldsymbol{x}(n) \triangleq [x_1(n), x_2(n), \cdots, x_M(n)]^T$, $\boldsymbol{w}_x(n) \triangleq [w_{x_1}(n), w_{x_2}(n), \cdots, w_{x_M}(n)]^T$, $\boldsymbol{s}(n) \triangleq [s_1(n), s_2(n), \cdots, s_p(n)]^T$, $\boldsymbol{A}(\theta) \triangleq [\boldsymbol{a}(\theta_1), \boldsymbol{a}(\theta_2), \cdots, \boldsymbol{a}(\theta_p)]$, $\boldsymbol{a}(\theta_k) \triangleq [1, e^{j\alpha_k}, \cdots, e^{j(M-1)\alpha_k}]^T$, $\boldsymbol{A}(\phi) \triangleq [\boldsymbol{a}(\phi_1), \boldsymbol{a}(\phi_2), \cdots, \boldsymbol{a}(\phi_p)]$, $\boldsymbol{a}(\phi_k) \triangleq [e^{j\beta_k}, e^{j2\beta_k}, \cdots, e^{jM\beta_k}]^T$, $\alpha_k \triangleq 2\pi d \cos\theta_k/\lambda$, and $\beta_k \triangleq 2\pi d \cos\phi_k/\lambda$. The relationship between the elevation angle θ_k, the azimuth angle ϕ_k and the projected azimuth angle $\bar{\phi}_k$ illustrated in Fig. 1 is given by $\cos\phi_k = \cos\bar{\phi}_k \sin\theta_k$.

In this paper, we make the following basic assumptions on the data model, which are similar to that in [10].

- A1) The array is calibrated, and the sensor spacing d of each ULA and that between the sensors z_0 and x_1 satisfy $0 < d \le \lambda/2$ for avoiding angle ambiguity problems.
- A2) For the simplicity of theoretical performance analysis, the incident signals $\{s_k(n)\}$ are temporally complex white Gaussian random processes with zero-mean and the variance given by $E\{s_k(n)s_k^*(t)\} = r_{s_k}\delta_{n,t}$ and $E\{s_k(n)s_k(t)\} = 0\ \forall n, t$, where $E\{\cdot\}$, $(\cdot)^*$, and $\delta_{n,t}$ denote the statistical expectation, the complex conjugate, and Kronecker delta.
- A3) The additive noises $\{w_{z_i}(n)\}$ and $\{w_{x_i}(n)\}$ are temporally and spatially complex white Gaussian random processes with zero-mean and the covariance matrices $E\{\boldsymbol{w}_z(n)\boldsymbol{w}_z^H(t)\} = E\{\boldsymbol{w}_x(n)\boldsymbol{w}_x^H(t)\} = \sigma^2\boldsymbol{I}_M\delta_{n,t}$ and $E\{\boldsymbol{w}_z(n)\boldsymbol{w}_z^T(t)\} = E\{\boldsymbol{w}_x(n)\boldsymbol{w}_x^T(t)\} = \boldsymbol{O}_{M\times M}, \forall n, t$, while they are statistically independent with each other, i.e., $E\{\boldsymbol{w}_x(n)\boldsymbol{w}_z^H(t)\} = \boldsymbol{O}_{M\times M}$, where $\boldsymbol{I}_m$, $\boldsymbol{O}_{m\times q}$, and $(\cdot)^H$ indicate the $m \times m$ identity matrix, the $m \times q$ null matrix, and Hermitian transpose. And the additive noise at each sensor of two ULAs along the z and x axes is uncorrelated with the incident signals.
- A4) The number of incident signals p is known or is estimated by the existing number detection techniques in advance (cf. [11]), and it satisfies the inequality that $p < M$ for an array of M.

In this paper, we deal with the problem of estimating the elevation and azimuth angles and pairing their estimates in a computationally effective and efficient way and analyze the statistical performance of the proposed 1-D DOA estimation with the available array data.

III. CODE Method Without Eigendecomposition

A. 1-D Estimation of Azimuth Angle

Under the assumptions of data model, from (1) and (2), we easily obtain the cross-correlation matrix $\boldsymbol{R}_{xz}$ between the received data of two ULAs along the x and z axes as

$$\begin{aligned}\boldsymbol{R}_{xz} &\triangleq E\left\{\boldsymbol{x}(n)\boldsymbol{z}^H(n)\right\} \\ &= \boldsymbol{A}(\phi)E\left\{\boldsymbol{s}(n)\boldsymbol{s}^H(n)\right\}\boldsymbol{A}^H(\theta) + E\left\{\boldsymbol{w}_x(n)\boldsymbol{w}_z^H(n)\right\} \\ &= \boldsymbol{A}(\phi)\boldsymbol{R}_s\boldsymbol{A}^H(\theta)\end{aligned} \tag{3}$$

where $\boldsymbol{R}_s$ is the source signal covariance matrix defined by $\boldsymbol{R}_s \triangleq E\{\boldsymbol{s}(n)\boldsymbol{s}^H(n)\}$. From (2), we have another signal vector $\bar{\boldsymbol{x}}(n)$ of the ULA along the x axis in backward and conjugate way

$$\begin{aligned}\bar{\boldsymbol{x}}(n) &\triangleq [x_M(n), \cdots, x_2(n), x_1(n)]^H = \boldsymbol{J}_M\boldsymbol{x}^*(n) \\ &= \boldsymbol{A}(\phi)\boldsymbol{D}^{-(M+1)}(\phi)\boldsymbol{s}^*(n) + \bar{\boldsymbol{w}}_x(n)\end{aligned} \tag{4}$$

where $\bar{\boldsymbol{w}}_x(n) \triangleq [w_{x_M}(n), \cdots, w_{x_2}(n), w_{x_1}(n)]^H$, $\boldsymbol{D}(\phi) \triangleq \mathrm{diag}(e^{j\beta_1}, e^{j\beta_2}, \cdots, e^{j\beta_p})$, and $\boldsymbol{J}_M$ is an $M \times M$ counteridentity matrix. Similarly from (1) and (4), we can get another cross-correlation matrix $\bar{\boldsymbol{R}}_{xz}$ between the received data of two ULAs as

$$\begin{aligned}\bar{\boldsymbol{R}}_{xz} &\triangleq E\left\{\bar{\boldsymbol{x}}(n)\boldsymbol{z}^T(n)\right\} \\ &= \boldsymbol{A}(\phi)\boldsymbol{D}^{-(M+1)}(\phi)\left(E\left\{\boldsymbol{s}(n)\boldsymbol{s}^H(n)\right\}\right)^*\boldsymbol{A}^T(\theta) \\ &\quad + E\left\{\bar{\boldsymbol{w}}_x^*(n)\boldsymbol{w}_z^T(n)\right\} \\ &= \boldsymbol{A}(\phi)\boldsymbol{D}^{-(M+1)}(\phi)\boldsymbol{R}_s^*\boldsymbol{A}^T(\theta) = \boldsymbol{J}_M\boldsymbol{R}_{xz}^*.\end{aligned} \tag{5}$$

Obviously the matrices $\boldsymbol{R}_{xz}$ in (3) and $\bar{\boldsymbol{R}}_{xz}$ in (5) are not affected by the additive noises of two ULAs. Then by combining these matrices together, we can form one $M \times 2M$ extended cross-correlation matrix $\boldsymbol{R}_x$ as

$$\begin{aligned}\boldsymbol{R}_x &\triangleq \left[\boldsymbol{R}_{xz}, \bar{\boldsymbol{R}}_{xz}\right] = \left[\boldsymbol{R}_{xz}, \boldsymbol{J}_M\boldsymbol{R}_{xz}^*\right] \\ &= \boldsymbol{A}(\phi)\left[\boldsymbol{R}_s\boldsymbol{A}^H(\theta), \boldsymbol{D}^{-(M+1)}(\phi)\boldsymbol{R}_s^*\boldsymbol{A}^T(\theta)\right].\end{aligned} \tag{6}$$

From Assumption A4 (i.e., $p < M$), we can divide $\boldsymbol{A}(\phi)$ in (2) into two submatrices in the downward direction as

$$\boldsymbol{A}(\phi) \triangleq \begin{bmatrix}\boldsymbol{A}_1(\phi) \\ \boldsymbol{A}_2(\phi)\end{bmatrix}\begin{matrix}\}p \\ \}M-p\end{matrix} \tag{7}$$

where $\boldsymbol{A}_1(\phi)$ and $\boldsymbol{A}_2(\phi)$ are the $p \times p$ and $(M-p) \times p$ submatrices consisting of the first p and the last $M-p$ rows of $\boldsymbol{A}(\phi)$ in (2), while their columns are given by $\boldsymbol{a}_1(\phi_k) \triangleq [e^{j\beta_k}, e^{j2\beta_k}, \cdots, e^{jp\beta_k}]^T$ and $\boldsymbol{a}_2(\phi_k) \triangleq [e^{j(p+1)\beta_k}, e^{j(p+2)\beta_k}, \cdots, e^{jM\beta_k}]^T$. Since the array response matrix $\boldsymbol{A}(\phi)$ is the Vandermonde matrix with full rank under Assumption A1, clearly $\boldsymbol{A}_1(\phi)$ has full rank, and the rows of $\boldsymbol{A}_2(\phi)$ can be expressed as a linear combination of linearly independent rows of $\boldsymbol{A}_1(\phi)$; equivalently there is a $p \times (M-p)$ linear operator $\boldsymbol{P}_x$ between $\boldsymbol{A}_1(\phi)$ and $\boldsymbol{A}_2(\phi)$ [9]

$$\boldsymbol{A}_2(\phi) = \boldsymbol{P}_x^H\boldsymbol{A}_1(\phi). \tag{8}$$

By using (7) and (8), the matrix $\boldsymbol{R}_x$ in (6) can be partitioned into two submatrices as

$$\begin{aligned}\bar{\boldsymbol{R}}_x &= \begin{bmatrix}\boldsymbol{A}_1(\phi)\\ \boldsymbol{P}_x^H\boldsymbol{A}_1(\phi)\end{bmatrix}\left[\bar{\boldsymbol{R}}_s\boldsymbol{A}^H(\theta), \bar{\boldsymbol{D}}^{-(M+1)}(\phi)\bar{\boldsymbol{R}}_s^*\boldsymbol{A}^T(\theta)\right]\\ &\triangleq \begin{bmatrix}\bar{\boldsymbol{R}}_{x1}\\ \boldsymbol{R}_{x2}\end{bmatrix}\begin{matrix}\}p\\ \}M-p\end{matrix}\\ &= \begin{bmatrix}\boldsymbol{R}_{xz1}, \bar{\boldsymbol{R}}_{xz1}\\ \boldsymbol{R}_{xz2}, \bar{\boldsymbol{R}}_{xz2}\end{bmatrix}\begin{matrix}\}p\\ \}M-p\end{matrix}\end{aligned} \tag{9}$$

where $\boldsymbol{R}_{x1}$ and $\boldsymbol{R}_{x2}$ consist of the first p rows and the last $M-p$ rows of the matrix $\boldsymbol{R}_x$, and $\boldsymbol{P}_x^H\boldsymbol{R}_{x1} = \boldsymbol{R}_{x2}$, while similarly $\boldsymbol{R}_{xz1}$ (or $\bar{\boldsymbol{R}}_{xz1}$) and $\boldsymbol{R}_{xz2}$ (or $\bar{\boldsymbol{R}}_{xz2}$) consist of the first p rows and the last $M-p$ rows of the matrix $\boldsymbol{R}_{xz}$ in (3) (or $\bar{\boldsymbol{R}}_{xz}$ in (5)). Hence the linear operator $\bar{\boldsymbol{P}}_x$ in (8) can be found from $\bar{\boldsymbol{R}}_{x1}$ and $\boldsymbol{R}_{x2}$ as [10]

$$\boldsymbol{P}_x = \boldsymbol{A}_1^{-H}(\phi)\boldsymbol{A}_2^H(\phi) = \left(\boldsymbol{R}_{x1}\boldsymbol{R}_{x1}^H\right)^{-1}\boldsymbol{R}_{x1}\boldsymbol{R}_{x2}^H. \tag{10}$$

Further by defining the matrix $\boldsymbol{Q}_x \triangleq [\boldsymbol{P}_x^T, -\boldsymbol{I}_{M-p}]^T$, from (8), we can get $\boldsymbol{Q}_x^H\boldsymbol{A}(\phi) = \boldsymbol{O}_{(M-p)\times p}$, which can be used to estimate the azimuth angles $\{\phi_k\}_{k=1}^p$ in the SUMWE-like manner.

Thus when the number of snapshots is finite, the azimuth angles $\{\phi_k\}_{k=1}^p$ can be estimated by minimizing the following cost function

$$f(\phi) = \boldsymbol{a}^H(\phi)\hat{\boldsymbol{\Pi}}_x\boldsymbol{a}(\phi) \tag{11}$$

where

$$\begin{aligned}\hat{\boldsymbol{\Pi}}_x &\triangleq \hat{\boldsymbol{Q}}_x\left(\hat{\boldsymbol{Q}}_x^H\hat{\boldsymbol{Q}}_x\right)^{-1}\hat{\boldsymbol{Q}}_x^H\\ &= \hat{\boldsymbol{Q}}_x\left(\boldsymbol{I}_{M-p} - \hat{\boldsymbol{P}}_x^H\left(\hat{\boldsymbol{P}}_x\hat{\boldsymbol{P}}_x^H + \boldsymbol{I}_p\right)^{-1}\hat{\boldsymbol{P}}_x\right)\hat{\boldsymbol{Q}}_x^H\end{aligned} \tag{12}$$

$$\hat{\boldsymbol{P}}_x = \left(\hat{\boldsymbol{R}}_{x1}\hat{\boldsymbol{R}}_{x1}^H\right)^{-1}\hat{\boldsymbol{R}}_{x1}\hat{\boldsymbol{R}}_{x2}^H \tag{13}$$

while $\hat{\boldsymbol{Q}}_x = [\hat{\boldsymbol{P}}_x^T, -\boldsymbol{I}_{M-p}]^T$, and $\hat{\boldsymbol{\Pi}}_x$ is calculated using the matrix inversion lemma implicitly [10], while the orthonormalization of the matrix $\hat{\boldsymbol{Q}}_x$ is used in $\hat{\boldsymbol{\Pi}}_x$ to improve the estimation performance [9], and $\hat{x}$ denotes the estimate of the variable x.

B. 1-D Estimation of Elevation Angle

From (1), we can define another signal vector $\bar{\boldsymbol{z}}(n)$ of the ULA along the z axis as

$$\begin{aligned}\bar{\boldsymbol{z}}(n) &\triangleq [z_{M-1}(n), \cdots, z_1(n), z_0(n)]^H = \boldsymbol{J}_M\boldsymbol{z}^*(n)\\ &= \boldsymbol{A}(\theta)\boldsymbol{D}^{-(M-1)}(\theta)\boldsymbol{s}^*(n) + \bar{\boldsymbol{w}}_z(n)\end{aligned} \tag{14}$$

where $\bar{\boldsymbol{w}}_z(n) \triangleq [w_{z_{M-1}}(n), \cdots, w_{z_1}(n), w_{z_0}(n)]^H$, and $\boldsymbol{D}(\theta) \triangleq \mathrm{diag}(e^{j\alpha_1}, e^{j\alpha_2}, \cdots, e^{j\alpha_p})$. Then from (14) and (2), we can obtain another cross-correlation matrix $\bar{\boldsymbol{R}}_{zx}$ between the received data of the ULAs along the z and x axes as

$$\begin{aligned}\bar{\boldsymbol{R}}_{zx} &\triangleq E\left\{\bar{\boldsymbol{z}}(n)\boldsymbol{x}^T(n)\right\}\\ &= \boldsymbol{A}(\theta)\boldsymbol{D}^{-(M-1)}(\theta)\left(E\left\{\boldsymbol{s}(n)\boldsymbol{s}^H(n)\right\}\right)^*\boldsymbol{A}^T(\phi)\\ &\quad + E\left\{\bar{\boldsymbol{w}}_z^*(n)\boldsymbol{w}_x^T(n)\right\}\\ &= \boldsymbol{A}(\theta)\boldsymbol{D}^{-(M-1)}(\theta)\boldsymbol{R}_s^*\boldsymbol{A}^T(\phi) = \boldsymbol{J}_M\boldsymbol{R}_{xz}^T.\end{aligned} \tag{15}$$

From (3) and (15), we can form a new $M\times 2M$ extended cross-correlation matrix $\boldsymbol{R}_z$ as

$$\begin{aligned}\boldsymbol{R}_z &\triangleq \left[\boldsymbol{R}_{xz}^H, \bar{\boldsymbol{R}}_{zx}\right] = \left[\boldsymbol{R}_{xz}^H, \boldsymbol{J}_M\boldsymbol{R}_{xz}^T\right]\\ &= \boldsymbol{A}(\theta)\left[\boldsymbol{R}_s\boldsymbol{A}^H(\phi), \boldsymbol{D}^{-(M-1)}(\theta)\boldsymbol{R}_s^*\boldsymbol{A}^T(\phi)\right].\end{aligned} \tag{16}$$

In the similar way to the estimation of azimuth angle described above, by dividing the matrix $\boldsymbol{R}_z$ in (16) into two submatrices as

$$\begin{aligned}\boldsymbol{R}_z &= \begin{bmatrix}\boldsymbol{A}_1(\theta)\\ \boldsymbol{A}_2(\theta)\end{bmatrix}\left[\boldsymbol{R}_s\boldsymbol{A}^H(\phi), \boldsymbol{D}^{-(M-1)}(\theta)\boldsymbol{R}_s^*\boldsymbol{A}^T(\phi)\right]\\ &\triangleq \begin{bmatrix}\boldsymbol{R}_{z1}\\ \boldsymbol{R}_{z2}\end{bmatrix}\begin{matrix}\}p\\ \}M-p\end{matrix}\end{aligned} \tag{17}$$

where $\boldsymbol{A}_1(\theta)$ and $\boldsymbol{A}_2(\theta)$ (or $\boldsymbol{R}_{z1}$ and $\boldsymbol{R}_{z2}$) consist of the first p and the last $M-p$ rows of $\boldsymbol{A}(\theta)$ in (1) [or $\boldsymbol{R}_z$ in (16)]. Then we can also obtain a new relation with the $p\times(M-p)$ linear operator $\boldsymbol{P}_z$ as $\boldsymbol{P}_z^H\boldsymbol{R}_{z_1} = \boldsymbol{R}_{z_2}$. As a result, the elevation angles $\{\theta_k\}_{k=1}^p$ can be estimated by minimizing the following cost function

$$f(\theta) = \boldsymbol{a}^H(\theta)\hat{\boldsymbol{\Pi}}_z\boldsymbol{a}(\theta) \tag{18}$$

where

$$\begin{aligned}\hat{\boldsymbol{\Pi}}_z &\triangleq \hat{\boldsymbol{Q}}_z\left(\hat{\boldsymbol{Q}}_z^H\hat{\boldsymbol{Q}}_z\right)^{-1}\hat{\boldsymbol{Q}}_z^H\\ &= \hat{\boldsymbol{Q}}_z\left(\boldsymbol{I}_{M-p} - \hat{\boldsymbol{P}}_z^H\left(\hat{\boldsymbol{P}}_z\hat{\boldsymbol{P}}_z^H + \boldsymbol{I}_p\right)^{-1}\hat{\boldsymbol{P}}_z\right)\hat{\boldsymbol{Q}}_z^H\end{aligned} \tag{19}$$

$$\hat{\boldsymbol{P}}_z = \left(\hat{\boldsymbol{R}}_{z1}\hat{\boldsymbol{R}}_{z1}^H\right)^{-1}\hat{\boldsymbol{R}}_{z1}\hat{\boldsymbol{R}}_{z2}^H \tag{20}$$

and $\hat{\boldsymbol{Q}}_z = [\hat{\boldsymbol{P}}_z^T, -\boldsymbol{I}_{M-p}]^T$.

C. Pair-Matching of Azimuth and Elevation Estimates

Since the estimated azimuth and elevation angles $\{\hat{\phi}_k\}_{k=1}^p$ and $\{\hat{\theta}_k\}_{k=1}^p$ are obtained independently, we should associate these estimates, when there are multiple incident signals. By combining the received signals at the ULAs along the z and x axes in (1) and (2), we define a new $2M\times 1$ combined vector $\boldsymbol{y}(n)$ as

$$\boldsymbol{y}(n) \triangleq \begin{bmatrix}\boldsymbol{x}(n)\\ \boldsymbol{z}(n)\end{bmatrix} = \boldsymbol{A}(\theta,\phi)\boldsymbol{s}(n) + \boldsymbol{w}_{xz}(n) \tag{21}$$

where $\boldsymbol{w}_{xz}(n) \triangleq [\boldsymbol{w}_x^T(n), \boldsymbol{w}_z^T(n)]^T$, and the $2M \times p$ extended array response matrix $\boldsymbol{A}(\theta, \phi)$ is given by

$$\boldsymbol{A}(\theta,\phi) \triangleq \begin{bmatrix} \boldsymbol{A}(\phi) \\ \boldsymbol{A}(\theta) \end{bmatrix} = \begin{bmatrix} \boldsymbol{A}_1(\phi) \\ \boldsymbol{A}_2(\phi) \\ \boldsymbol{A}(\theta) \end{bmatrix} \begin{matrix} \}p \\ \}M-p \\ \end{matrix}. \tag{22}$$

Evidently we have $\text{rank}(\boldsymbol{A}(\theta,\phi)) = \text{rank}(\boldsymbol{A}(\phi)) = \text{rank}(\boldsymbol{A}(\theta)) = \text{rank}(\boldsymbol{A}_1(\phi)) = p$. This means that the last $2M-p$ rows of $\boldsymbol{A}(\theta,\phi)$ in (22) can be expressed as a linear combination of linearly independent rows of $\boldsymbol{A}_1(\phi)$, i.e.

$$\begin{bmatrix} \boldsymbol{A}_2(\phi) \\ \boldsymbol{A}(\theta) \end{bmatrix} = \boldsymbol{P}^H \boldsymbol{A}_1(\phi). \tag{23}$$

Further from (21), we obtain a $2M \times 2M$ covariance matrix of the combined signal vector $\boldsymbol{y}(n)$ of two ULAs as

$$\begin{aligned} \boldsymbol{R}_{yy} &\triangleq E\left\{\boldsymbol{y}(n)\boldsymbol{y}^H(n)\right\} = \begin{bmatrix} \boldsymbol{R}_{xx}, & \boldsymbol{R}_{xz} \\ \boldsymbol{R}_{xz}^H, & \boldsymbol{R}_{zz} \end{bmatrix} \\ &= \boldsymbol{A}(\theta,\phi)\boldsymbol{R}_s\boldsymbol{A}^H(\theta,\phi) + \sigma^2\boldsymbol{I}_{2M} \\ &\triangleq \begin{bmatrix} \boldsymbol{G}_1 \\ \boldsymbol{G}_2 \end{bmatrix} \begin{matrix} \}p \\ \}2M-p \end{matrix} \end{aligned} \tag{24}$$

where $\boldsymbol{R}_{xx}$ and $\boldsymbol{R}_{zz}$ are the covariance matrices of the array data of the ULA along the x or z axis given by $\boldsymbol{R}_{xx} \triangleq E\{\boldsymbol{x}(n)\boldsymbol{x}^H(n)\} = \boldsymbol{A}(\phi)\boldsymbol{R}_s\boldsymbol{A}^H(\phi) + \sigma^2\boldsymbol{I}_M$ and $\boldsymbol{R}_{zz} \triangleq E\{\boldsymbol{z}(n)\boldsymbol{z}^H(n)\} = \boldsymbol{A}(\theta)\boldsymbol{R}_s\boldsymbol{A}^H(\theta) + \sigma^2\boldsymbol{I}_M$, while $\boldsymbol{G}_1$ and $\boldsymbol{G}_2$ are two submatrices consisting of the first p and the last $2M-p$ columns of the matrix $\boldsymbol{R}_{yy}$ in (24). Hence we can find that the elevation angle θ_k and azimuth angle ϕ_k can be estimated by minimizing the following cost function:

$$f(\theta,\phi) = \boldsymbol{a}^H(\theta,\phi)\hat{\boldsymbol{\Pi}}\boldsymbol{a}(\theta,\phi) \tag{25}$$

where $\hat{\boldsymbol{\Pi}} \triangleq \hat{\boldsymbol{Q}}(\boldsymbol{I}_{2M-p} - \hat{\boldsymbol{P}}^H(\hat{\boldsymbol{P}}\hat{\boldsymbol{P}}^H + \boldsymbol{I}_p)^{-1}\hat{\boldsymbol{P}})\hat{\boldsymbol{Q}}^H$, $\hat{\boldsymbol{P}} = (\hat{\boldsymbol{G}}_1\hat{\boldsymbol{G}}_1^H)^{-1}\hat{\boldsymbol{G}}_1\hat{\boldsymbol{G}}_2^H$, and $\hat{\boldsymbol{Q}} = [\hat{\boldsymbol{P}}^T, -\boldsymbol{I}_{2M-p}]^T$.

Therefore from (25), the estimated parameters $\{\hat{\phi}_k\}_{k=1}^p$ and $\{\hat{\theta}_k\}_{k=1}^p$ can be associated by

$$\{i, k_i\} = \min_{k_i} f\left(\hat{\theta}_i, \hat{\phi}_{k_i}\right), \text{ subject to } k_i \neq k_m \tag{26}$$

for $m = 1, 2, \cdots, i-1$ and $i = 1, 2, \cdots, p$. Now the pairing process is accomplished by repeating the above minimization for $i = 1, 2, \cdots, p$, where the ith elevation estimate $\hat{\theta}_i$ is associated with the k_ith azimuth estimate $\hat{\phi}_{k_i}$, and the constraint condition $k_i \neq k_m$ for $m = 1, 2, \cdots, i-1$ is to avoid the different $\hat{\theta}_k$ associate with the same $\hat{\phi}_k$.

D. Implementation of Proposed Method

As shown in (6) and (16), the elevation and azimuth angles are estimated independently by using the 1-D subspace-based technique from the matrices formed from the cross-correlation matrix $\boldsymbol{R}_{xz}$ of two ULAs along the x and z axes, whereas the covariance matrices $\boldsymbol{R}_{xx}$ and $\boldsymbol{R}_{zz}$ of two ULAs are required only for pair-matching of the estimated elevation and azimuth angles, where the computational burdensome eigendecompsotion is not needed, and the effect of additive noises is mitigated in the DOA estimation. Based on the above analysis, when the N snapshots of array data $\{\boldsymbol{x}(n), \boldsymbol{z}(n)\}_{n=1}^N$ are available, the proposed CODE method can be implemented as follows:

1) Calculate the estimate of the covariance matrix $\boldsymbol{R}_{yy}$ in (24) as

$$\hat{\boldsymbol{R}}_{yy} = \begin{bmatrix} \hat{\boldsymbol{R}}_{xx}, & \hat{\boldsymbol{R}}_{xz} \\ \hat{\boldsymbol{R}}_{xz}^H, & \hat{\boldsymbol{R}}_{zz} \end{bmatrix} = \frac{1}{N}\sum_{n=1}^N \boldsymbol{y}(n)\boldsymbol{y}^H(n). \tag{27}$$

.... $32M^2N$ flops

2) Form the estimates of the correlation matrices $\boldsymbol{R}_x$ in (6) and $\boldsymbol{R}_z$ in (16) from $\hat{\boldsymbol{R}}_{yy}$ in (27) as

$$\hat{\boldsymbol{R}}_x = \left[\hat{\boldsymbol{R}}_{xz}, \boldsymbol{J}_M\hat{\boldsymbol{R}}_{xz}^*\right] \tag{28}$$

$$\hat{\boldsymbol{R}}_z = \left[\hat{\boldsymbol{R}}_{xz}^H, \boldsymbol{J}_M\hat{\boldsymbol{R}}_{xz}^T\right]. \tag{29}$$

3) Calculate the estimated orthogonal projectors $\hat{\boldsymbol{\Pi}}_x$ by using (12) and (13) and $\hat{\boldsymbol{\Pi}}_z$ by using (19) and (20).

.... $2(16Mp^2 + 16Mp(M-p) + 24p^2(M-p) + 8p(M-p)^2 + 8M(M-p)^2 + 8M^2(M-p) + 2p^2 + 2(M-p)^2 + O(p^3))$ flops

4) Estimate the azimuth and elevation angles ϕ_k and θ_k by finding the phases of the p zeros of the polynomial $p_\theta(z)$ and $p_\phi(z)$ using (11) and (18), where $p_\phi(z) \triangleq z^{M-1}\boldsymbol{p}^H(z)\hat{\boldsymbol{\Pi}}_x\boldsymbol{p}(z)$, and $p_\theta(z) \triangleq z^{M-1}\boldsymbol{p}^H(z)\hat{\boldsymbol{\Pi}}_z\boldsymbol{p}(z)$, while $\boldsymbol{p}(z) \triangleq [1, z, \cdots, z^{M-1}]^T$, and $z \triangleq e^{j2\pi d\cos\phi/\lambda}$ or $z \triangleq e^{j2\pi d\cos\theta/\lambda}$.

.... $2\left((M-1)^2 + O(2M-1)^3\right)$ flops

5) Perform the pairing of the estimated azimuth and elevation parameters by using (26).

.... $32M^2(2M-p) + 16M(2M-p)^2 + 16Mp(2M-p) + 16Mp^2 + 24p^2(2M-p) + 8p(2M-p)^2 + 2p^2 + 2(2M-p)^2 + O(p^3)$ flops

In above, the computational complexity of each step is roughly indicated in terms of the number of MATLAB flops, and the computational complexity is $32M^2N + 160M^3$ flops if $M \gg p$, which occurs often in application of DOA estimation.

Remark 1: Unlike the classical subspace-based direction estimation methods such as the MUSIC (multiple signal classification) [43], [47] and ESPRIT [32], some computationally simple subspace-based 1-D direction estimators without eigendecomposition such as the orthonormal PM (OPM) [9] and SUMWE [10] were proposed, where the null space is obtained through a linear propagator based on the partition of array response matrix similar to (7) and (8) and used to estimate the directions with a direction finding cost function similar to (11) [or (18)], and certainly they can be employed to each ULA of the L-shaped array along the x or z axis to estimate the azimuth or elevation angles independently. Essentially the estimation performance of these methods [9], [10] and the proposed CODE method is affected by the estimation of linear propagator and the working array aperture. By partitioning the covariance matrix $\boldsymbol{R}_{xx}$ (or $\boldsymbol{R}_{zz}$) of each ULA into two parts such as $\boldsymbol{R}_{xx} = [\underbrace{\boldsymbol{G}}_{p}, \underbrace{\boldsymbol{H}}_{M-p}]$, the OPM linear operator is estimated as $\hat{\boldsymbol{P}}_{\text{OPM}} = (\boldsymbol{G}^H\boldsymbol{G})^{-1}\boldsymbol{G}^H\boldsymbol{H}$ (i.e., [9,

Eq. (27)]). From (24), we can find that this LS estimate $\hat{\boldsymbol{P}}_{\mathrm{OPM}}$ is affected by the additive noise at each ULA and it results in worse estimation of ϕ_k (or θ_k), when the SNR is relatively low and/or the number of snapshots is small (cf. [9]). On the other hand, by decorrelating the coherency of incident signals with subarray averaging, the SUMWE linear propagator $\hat{\boldsymbol{P}}_{\mathrm{SUMWE}}$ is estimated from the combined Hankel correlation matrix formed by the cross-correlations of some sensor data of one ULA, where the influence of additive noise is alleviated. Unfortunately, the SUMWE may performs worse for the uncorrelated or correlated signals with small number of snapshot or at low SNR, because the working array aperture is reduced to $M-p$ due to subarray averaging and only $2(M-1)$ cross-correlations of one ULA is used in the estimation $\hat{\boldsymbol{P}}_{\mathrm{SUMWE}}$. However, since the maximum working array aperture (i.e., M) is used in direction finding, and all cross-correlations between two ULAs of the L-shaped array along the x and z axes are effectively exploited in the LS estimation $\hat{\boldsymbol{P}}_x$ in (13) (or $\hat{\boldsymbol{P}}_z$ in (20), where the influence of additive noises is sufficiently mitigated, and the proposed CODE method outperforms the OPM and SUMWE in the estimation of azimuth and elevation angles. □

IV. Statistical Analysis

The performance of the 2-D DOA estimator is usually affected by the 1-D estimation of the elevation and azimuth angles itself and the pair-matching of estimated elevation and azimuth angles. Here we study the statistical performance of the proposed CODE method for 1-D elevation or azimuth estimation for large number of snapshots.

When the number of snapshots N is sufficiently large, firstly we can find that the estimated azimuth and elevation angles $\hat{\phi}_k$ and $\hat{\theta}_k$ obtained by (11) and (18) are consistent with the following Lemma on the consistency of the CODE estimates.

Lemma: As the number of snapshots N tends to infinity, the estimated azimuth and elevation angles $\hat{\phi}_k$ and $\hat{\theta}_k$ obtained by minimizing the cost functions $f(\phi)$ in (11) and $f(\theta)$ in (18) approach the true parameters ϕ_k and θ_k with probability one (w.p.1).

Proof: See Appendix A. ■

From this Lemma, we can obtain the asymptotic MSE expressions of these estimates $\hat{\phi}_k$ and $\hat{\theta}_k$ as follows.

Theorem 1: The large-sample MSEs of the estimates $\hat{\phi}_k$ and $\hat{\theta}_k$ obtained by (11) and (18) are given by

$$\begin{aligned}\mathrm{MSE}(\hat{\phi}_k) &\triangleq E\left\{(\hat{\phi}_k-\phi_k)^2\right\}\\ &=\frac{\sigma^2}{2NH_{xkk}^2}\mathrm{Re}\Big\{H_{xkk}\boldsymbol{h}^H(\phi_k)\boldsymbol{R}_{zz}\boldsymbol{h}(\phi_k)\\ &\quad+2\boldsymbol{g}^H(\phi_k)\boldsymbol{J}_M\boldsymbol{g}^*(\phi_k)\bar{\boldsymbol{h}}^T(\phi_k)\boldsymbol{R}_{zz}\boldsymbol{h}(\phi_k)\\ &\quad+H_{xkk}\bar{\boldsymbol{h}}^T(\phi_k)\,\boldsymbol{R}_{zz}\bar{\boldsymbol{h}}^*(\phi_k)\Big\} \qquad (30)\\ \mathrm{MSE}(\hat{\theta}_k) &\triangleq E\left\{(\hat{\theta}_k-\theta_k)^2\right\}\\ &=\frac{\sigma^2}{2NH_{zkk}^2}\mathrm{Re}\Big\{H_{zkk}\boldsymbol{h}^H(\theta_k)\boldsymbol{R}_{xx}\boldsymbol{h}(\theta_k)\\ &\quad+2\boldsymbol{g}^H(\theta_k)\boldsymbol{J}_M\boldsymbol{g}^*(\theta_k)\bar{\boldsymbol{h}}^T(\theta_k)\boldsymbol{R}_{xx}\boldsymbol{h}(\theta_k)\\ &\quad+H_{zkk}\bar{\boldsymbol{h}}^T(\theta_k)\,\boldsymbol{R}_{xx}\bar{\boldsymbol{h}}^*(\theta_k)\Big\} \qquad (31)\end{aligned}$$

where $\boldsymbol{g}(\phi_k)\triangleq\bar{\boldsymbol{\Pi}}_x\boldsymbol{d}(\phi_k)$, $H_{xkk}\triangleq\boldsymbol{d}^H(\phi_k)\bar{\boldsymbol{\Pi}}_x\boldsymbol{d}(\phi_k)$, $\boldsymbol{d}(\phi_k)\triangleq d(\boldsymbol{a}(\phi))/(d\phi)|_{\phi=\phi_k}$, $\boldsymbol{h}(\phi_k)\triangleq\boldsymbol{R}_{xz1}^H(\boldsymbol{R}_{x1}\boldsymbol{R}_{x1}^H)^{-1}\cdot\boldsymbol{a}_1(\phi_k)$, and $\bar{\boldsymbol{h}}(\phi_k)\triangleq\bar{\boldsymbol{R}}_{xz1}^H(\boldsymbol{R}_{x1}\boldsymbol{R}_{x1}^H)^{-1}\boldsymbol{a}_1(\phi_k)$, while $\boldsymbol{g}(\theta_k)\triangleq\bar{\boldsymbol{\Pi}}_z\boldsymbol{d}(\theta_k)$, $H_{zkk}\triangleq\boldsymbol{d}^H(\theta_k)\bar{\boldsymbol{\Pi}}_z\boldsymbol{d}(\theta_k)$, $\boldsymbol{d}(\theta_k)\triangleq d(\boldsymbol{a}(\theta))/(d\theta)|_{\theta=\theta_k}$, $\boldsymbol{h}(\theta_k)\triangleq\boldsymbol{R}_{zx1}^H(\boldsymbol{R}_{z1}\boldsymbol{R}_{z1}^H)^{-1}\boldsymbol{a}_1(\theta_k)$, and $\bar{\boldsymbol{h}}(\theta_k)\triangleq\bar{\boldsymbol{R}}_{zx1}^H(\boldsymbol{R}_{z1}\boldsymbol{R}_{z1}^H)^{-1}\boldsymbol{a}_1(\theta_k)$.

Proof: See Appendix B. ■

V. Numerical Examples

In this section, we verify the estimation and pairing performances of the proposed method and the theoretical analysis of the statistical property of the proposed 1-D DOA estimation through some numerical examples. Each ULA of the L-shaped array has $M=7$ sensors with half-wavelength spacing, and the SNR is defined as the ratio of the signal power to the noise variance at each sensor. In the simulations, the subspace-based 1-D DOA estimators such as the root-MUSIC [43], [44], [47], the OPM [9] and the SUMWE [10] and the 2-D DOA estimation methods such as the MPM [3] and the JVSD [5] for the L-shaped array are carried out for comparing the performance of direction estimation, where the correct pairing is used in these methods except for the JSVD, while the CCM-based pair-matching with the ESPRIT 1-D DOA estimation (referred as CCM-ESPRIT) [4] is also conducted for comparing the performance comparisons of direction estimation and successful pair-matching. All the results shown below are obtained from 1000 independent trials.

Firstly we briefly review the 2-D DOA estimation techniques such as the MPM [3] and the JSVD [5] and the CCM-based pair-matching [4] for the L-shaped array in the $x-z$ plane for better understanding of the performance comparison. Then the effectiveness of the proposed CODE method and the validity of statistical analysis are demonstrated.

1) Review of MPM [3]: By dividing the ULA along the x axis into two forward overlapping subarrays with $M-1$ sensors and letting $\bar{\boldsymbol{A}}(\phi)$ be the subarray response matrix, which consists of the first $M-1$ rows of $\boldsymbol{A}(\phi)$, from (2), the received signals of these subarrays are expressed by

$$\begin{aligned}\boldsymbol{x}_{f1}(n)&\triangleq[x_1(n),x_2(n),\cdots,x_{M-1}(n)]^T\\ &=\bar{\boldsymbol{A}}(\phi)\boldsymbol{s}(n)+\boldsymbol{w}_{xf1}(n) \qquad (32)\\ \boldsymbol{x}_{f2}(n)&\triangleq[x_2(n),x_3(n),\cdots,x_M(n)]^T\\ &=\bar{\boldsymbol{A}}(\phi)\boldsymbol{D}(\phi)\boldsymbol{s}(n)+\boldsymbol{w}_{xf2}(n) \qquad (33)\end{aligned}$$

where $\boldsymbol{w}_{xf1}(n)\triangleq[w_{x_1}(n),w_{x_2}(n),\cdots,w_{x_{M-1}}(n)]^T$, $\boldsymbol{w}_{xf2}(n)\triangleq[w_{x_2}(n),w_{x_3}(n),\cdots,w_{x_M}(n)]^T$, and the $(M-1)\times p$ matrix $\bar{\boldsymbol{A}}(\phi)$ can be partitioned as

$$\bar{\boldsymbol{A}}(\phi)\triangleq\begin{bmatrix}\boldsymbol{A}_1(\phi)\\ \bar{\boldsymbol{A}}_2(\phi)\end{bmatrix}\begin{matrix}\}p\\ \}M-1-p\end{matrix}. \qquad (34)$$

Then a $2(M-1)\times 1$ signal vector is formed as

$$\boldsymbol{x}_f(n)\triangleq\begin{bmatrix}\boldsymbol{x}_{f1}(n)\\ \boldsymbol{x}_{f2}(n)\end{bmatrix}=\boldsymbol{C}(\phi)\boldsymbol{s}(n)+\boldsymbol{w}_{xf}(n) \qquad (35)$$

where $\boldsymbol{w}_{xf}(n) \triangleq [\boldsymbol{w}_{xf1}^T(n), \boldsymbol{w}_{xf2}^T(n)]^T$, and the $2(M-1)\times p$ combined array response matrix $\boldsymbol{C}(\phi)$ is given by

$$\boldsymbol{C}(\phi) \triangleq \begin{bmatrix} \bar{\boldsymbol{A}}(\phi) \\ \bar{\boldsymbol{A}}(\phi)\boldsymbol{D}(\phi) \end{bmatrix} = \begin{bmatrix} \boldsymbol{A}_1(\phi) \\ \boldsymbol{C}_1(\phi) \end{bmatrix} \begin{matrix} \}p \\ \}2(M-1)-p \end{matrix} \tag{36}$$

with $\boldsymbol{C}_1(\phi) \triangleq [\bar{\boldsymbol{A}}_2^T(\phi), (\bar{\boldsymbol{A}}(\phi)\boldsymbol{D}(\phi))^T]^T$. Clearly there is a $(2(M-1)-p)\times p$ linear propagator $\bar{\boldsymbol{P}}$ between $\boldsymbol{A}_1(\phi)$ and $\boldsymbol{C}_1(\phi)$ as [9]

$$\bar{\boldsymbol{P}}^H \boldsymbol{A}_1(\phi) = \boldsymbol{C}_1(\phi). \tag{37}$$

By dividing $\bar{\boldsymbol{P}}$ into three parts as follows:

$$\bar{\boldsymbol{P}}^H \triangleq \begin{bmatrix} \bar{\boldsymbol{P}}_1 \\ \bar{\boldsymbol{P}}_2 \\ \bar{\boldsymbol{P}}_3 \end{bmatrix} \begin{matrix} \}M-1-p \\ \}p \\ \}M-1-p \end{matrix} \tag{38}$$

and by substituting (38), (34), and (36) into (37), we easily get

$$\bar{\boldsymbol{P}}_1 \boldsymbol{A}_1(\phi) = \boldsymbol{A}_2(\phi) \tag{39}$$

$$\bar{\boldsymbol{P}}_2 \boldsymbol{A}_1(\phi) = \boldsymbol{A}_1(\phi)\boldsymbol{D}(\phi) \tag{40}$$

$$\bar{\boldsymbol{P}}_3 \boldsymbol{A}_1(\phi) = \boldsymbol{A}_2(\phi)\boldsymbol{D}(\phi). \tag{41}$$

Hence from (39) and (41), we have [3], [8]

$$\bar{\boldsymbol{P}}_1^{\#} \bar{\boldsymbol{P}}_3 = \boldsymbol{A}_1(\phi)\boldsymbol{D}(\phi)\boldsymbol{A}_1^{-1}(\phi). \tag{42}$$

This means that the azimuth angle ϕ_k (i.e., the diagonal element of $\boldsymbol{D}(\phi)$) can be estimated from the eigenvalue of $\bar{\boldsymbol{P}}_1^{\#}\bar{\boldsymbol{P}}_3$ in an ESPRIT-like manner (cf. [3], [32]), where $(\cdot)^{\#}$ denotes the pseudoinverse.

Further when the finite snapshots of array data are available, from (35) and (37), the linear propagator $\bar{\boldsymbol{P}}$ can be estimated from the $2(M-1)\times 2(M-1)$ sampled covariance matrix $\hat{\boldsymbol{R}}$ of combined received data $\{\boldsymbol{x}_f(n)\}$ of two overlapping forward subarrays as

$$\hat{\bar{\boldsymbol{P}}} = \left(\hat{\boldsymbol{R}}_1^H \hat{\boldsymbol{R}}_1\right)^{-1} \hat{\boldsymbol{R}}_1^H \hat{\boldsymbol{R}}_2 \tag{43}$$

where

$$\hat{\boldsymbol{R}} = \frac{1}{N}\sum_{n=1}^{N} \boldsymbol{x}_f(n)\boldsymbol{x}_f^H(n) \triangleq \Big[\underbrace{\hat{\boldsymbol{R}}_1}_{p}, \underbrace{\hat{\boldsymbol{R}}_2}_{2(M-1)-p}\Big]. \tag{44}$$

By performing the same procedure on the received data of the ULA on the z axis, the elevation angle θ_k can be also obtained (see [3] for details).

Remark 2: From (32), (33), and (35), by taking the expectation on both sides of (44), we can obtain that $E\{\hat{\boldsymbol{R}}\} = \boldsymbol{C}(\phi)\boldsymbol{R}_s\boldsymbol{C}^H(\phi) + \sigma^2[\boldsymbol{\Gamma}_1^T, \boldsymbol{\Gamma}_2^T]^T$, where $\boldsymbol{\Gamma}_1 \triangleq [\boldsymbol{I}_{M-1}, \boldsymbol{I}_{M-1}^{(-1)}]$, $\boldsymbol{\Gamma}_2 \triangleq [\boldsymbol{I}_{M-1}^{(+1)}, \boldsymbol{I}_{M-1}]$, $\boldsymbol{I}_m^{(\pm q)}$ denotes an $m\times m$ matrix with unity elements along the qth upper (for $+q$) or lower (for $-q$) diagonal off the major diagonal and zeros elsewhere. Evidently the estimate $\hat{\bar{\boldsymbol{P}}}$ in (43) (i.e., $\hat{\boldsymbol{P}}_{data}$ or $\hat{\boldsymbol{P}}_{csm}$ in [3, Eq. (17) or (18)]) is not the optimal solution of the linear propagator $\bar{\boldsymbol{P}}$ even when $N\to\infty$, and consequently the MPM [3] gives the estimate of elevation or azimuth angle with larger MSE regardless of SNR, though the ESPRIT-like manner is employed for estimating the azimuth or elevation angles with computationally cumbersome eigendecomposition. □

2) Review of JSVD [5]: By dividing the ULA along the z axis into two forward overlapping subarrays with $M-1$ sensors and letting $\bar{\boldsymbol{A}}(\theta)$ be the subarray response matrix, which consists of the first $M-1$ rows of $\boldsymbol{A}(\theta)$, from (1), the received signals of these subarrays are expressed by

$$\begin{aligned} \boldsymbol{z}_{f1}(n) &\triangleq [z_0(n), z_1(n), \cdots, z_{M-2}(n)]^T \\ &= \bar{\boldsymbol{A}}(\theta)\boldsymbol{s}(n) + \boldsymbol{w}_{zf1}(n) \end{aligned} \tag{45}$$

$$\begin{aligned} \boldsymbol{z}_{f2}(n) &\triangleq [z_1(n), z_2(n), \cdots, z_{M-1}(n)]^T \\ &= \bar{\boldsymbol{A}}(\theta)\boldsymbol{D}(\theta)\boldsymbol{s}(n) + \boldsymbol{w}_{xf2}(n) \end{aligned} \tag{46}$$

where $\boldsymbol{w}_{f1}(n) \triangleq [w_{z_0}(n), w_{z_1}(n), \cdots, w_{z_{M-2}}(n)]^T$, $\boldsymbol{w}_{f2}(n) \triangleq [w_{z_1}(n), w_{z_2}(n), \cdots, w_{z_{M-1}}(n)]^T$, and two $M\times(M-1)$ cross-correlation matrices $\bar{\boldsymbol{R}}_{xz1}$ and $\bar{\boldsymbol{R}}_{xz2}$ between $\boldsymbol{x}(n)$ in (2) and $\boldsymbol{z}_{f1}(n)$ in (45) or $\boldsymbol{z}_{f2}(n)$ in (46) are given by

$$\bar{\boldsymbol{R}}_{xz1} \triangleq E\left\{\boldsymbol{x}(n)\boldsymbol{z}_{f1}^H(n)\right\} = \boldsymbol{A}(\phi)\boldsymbol{R}_s\bar{\boldsymbol{A}}^H(\theta) \tag{47}$$

$$\bar{\boldsymbol{R}}_{xz2} \triangleq E\left\{\boldsymbol{x}(n)\boldsymbol{z}_{f2}^H(n)\right\} = \boldsymbol{A}(\phi)\boldsymbol{R}_s\boldsymbol{D}^H(\theta)\bar{\boldsymbol{A}}^H(\theta). \tag{48}$$

Then a $2M\times(M-1)$ combined cross-correlation matrix $\bar{\boldsymbol{R}}$ is formed as

$$\bar{\boldsymbol{R}} \triangleq \begin{bmatrix} \bar{\boldsymbol{R}}_{xz1} \\ \bar{\boldsymbol{R}}_{xz2} \end{bmatrix} = \begin{bmatrix} \boldsymbol{A}(\phi)\boldsymbol{R}_s \\ \boldsymbol{A}(\phi)\boldsymbol{R}_s\boldsymbol{D}^H(\theta) \end{bmatrix} \bar{\boldsymbol{A}}^H(\theta). \tag{49}$$

Based on the ideal treatment $\boldsymbol{R}_s\boldsymbol{D}^H(\theta) = \boldsymbol{D}^H(\theta)\boldsymbol{R}_s$ (i.e., $\boldsymbol{\Lambda\Omega} = \boldsymbol{\Omega\Lambda}$ in [5, Eqs. (8) and (9)]), $\bar{\boldsymbol{R}}$ in (49) is rewritten as

$$\bar{\boldsymbol{R}} = \begin{bmatrix} \boldsymbol{A}(\phi) \\ \boldsymbol{A}(\phi)\boldsymbol{D}^H(\theta) \end{bmatrix} \boldsymbol{R}_s\bar{\boldsymbol{A}}^H(\theta). \tag{50}$$

By performing the SVD on the matrix $\bar{\boldsymbol{R}}$ in (49) as $\bar{\boldsymbol{R}} = \boldsymbol{U\Sigma V}$, the following relation is obtained [32]:

$$\boldsymbol{U}_1 \triangleq \begin{bmatrix} \boldsymbol{U}_{11} \\ \boldsymbol{U}_{12} \end{bmatrix} \begin{matrix} \}M \\ \}M \end{matrix} = \begin{bmatrix} \boldsymbol{A}(\phi) \\ \boldsymbol{A}(\phi)\boldsymbol{D}^H(\theta) \end{bmatrix} \boldsymbol{T} \tag{51}$$

where $\boldsymbol{U}_1$ consists of the first p left singular vectors of $\bar{\boldsymbol{R}}$ (i.e., the first p columns of $\boldsymbol{U}$), and $\boldsymbol{T}$ is a $p\times p$ nonsingular matrix, and hence the elevation angles $\{\theta_k\}$ (i.e., the diagonal elements of $\boldsymbol{D}^H(\theta)$) can be estimated from the p eigenvalues of $\boldsymbol{U}_{11}^{\#}\boldsymbol{U}_{12}$ in an ESPRIT-like manner (cf. [5], [32]), while the azimuth angles $\{\phi_k\}$ can be estimated with a "beamforming-like" method by using $\boldsymbol{A}(\phi) = \boldsymbol{U}_{11}\boldsymbol{T}^{-1}$, where $\boldsymbol{T}^{-1}$ is made up of the p eigenvectors (see [5] for details).

Remark 3: In fact, the ideal treatment $\boldsymbol{R}_s\boldsymbol{D}^H(\theta) = \boldsymbol{D}^H(\theta)\boldsymbol{R}_s$ (i.e., $\boldsymbol{\Lambda\Omega} = \boldsymbol{\Omega\Lambda}$ in [5, Eqs. (8) and (9)]) is only valid when the source signal covariance matrix $\boldsymbol{R}_s$ is diagonal matrix. Consequently from (49), we can find that the ESPRIT-like relation $\boldsymbol{U}_{11} = \boldsymbol{A}(\phi)\boldsymbol{T}$ in (51) (i.e., [5, Eq. (16)]) for estimating the azimuth angles should be corrected to $\boldsymbol{U}_{11} = \boldsymbol{A}(\phi)\boldsymbol{R}_s\boldsymbol{T}$. Hence when the finite array data are available, the nonzero entries outside the main diagonal of the estimated source signal covariance matrix $\hat{\boldsymbol{R}}_s$ couple up $\{\boldsymbol{a}(\phi_k)\}$, and the estimate $\hat{\phi}_k$

is caused to be inaccurate even though the eigendecomposition is used. □

3) Review of CCM-Based Pair-Matching [4]: By reexpressing the array response matrices $\boldsymbol{A}(\theta)$ in (1) and $\boldsymbol{A}(\phi)$ in (2) as $\boldsymbol{A}(\theta) = [\boldsymbol{b}_0(\theta), \boldsymbol{b}_1(\theta), \cdots, \boldsymbol{b}_{M-1}(\theta)]^T$ and $\boldsymbol{A}(\phi) = [\boldsymbol{b}_1(\phi), \boldsymbol{b}_2(\phi), \cdots, \boldsymbol{b}_M(\phi)]^T$, where $\boldsymbol{b}_k(\theta) \triangleq [e^{jk\alpha_1}, e^{jk\alpha_2}, \cdots, e^{jk\alpha_p}]^T$ and $\boldsymbol{b}_k(\phi) \triangleq [e^{jk\beta_1}, e^{jk\beta_2}, \cdots, e^{jk\beta_p}]^T$, and defining a new signal vector $\tilde{\boldsymbol{x}}(n)$ as

$$\begin{aligned}\tilde{\boldsymbol{x}}(n) &\triangleq [z_0(n), x_1(n), \cdots, x_{M-1}(n)]^T \\ &= \tilde{\boldsymbol{A}}(\phi)\boldsymbol{s}(n) + \tilde{\boldsymbol{w}}(n)\end{aligned} \tag{52}$$

where $\tilde{\boldsymbol{A}}(\phi) \triangleq [\boldsymbol{b}_0(\phi), \boldsymbol{b}_1(\phi), \cdots, \boldsymbol{b}_{M-1}(\phi)]^T$ and $\tilde{\boldsymbol{w}}(n) \triangleq [w_{z_0}(n), w_{x_1}(n), \cdots, w_{x_{M-1}}(n)]^T$, from (52) and (1), we can obtain a new $M \times M$ correlation matrix $\tilde{\boldsymbol{R}}_{zx}$ as

$$\tilde{\boldsymbol{R}}_{zx} \triangleq E\left\{\boldsymbol{z}(n)\tilde{\boldsymbol{x}}^H(n)\right\} = \boldsymbol{A}(\theta)\boldsymbol{R}_s\tilde{\boldsymbol{A}}^H(\phi) + \sigma^2\tilde{\boldsymbol{I}}_M \tag{53}$$

where $\tilde{\boldsymbol{I}}_M \triangleq \mathrm{diag}(1, 0, \cdots, 0)$. Then the llth element $\tilde{r}_{ll}$ on the diagonal of $\tilde{\boldsymbol{R}}_{zx}$ in (53) is given by

$$\begin{aligned}\tilde{r}_{ll} &= \boldsymbol{b}_{l-1}^T(\theta)\boldsymbol{R}_s\boldsymbol{b}_{l-1}^*(\phi) + \sigma^2\delta_{l,1} \\ &= \sum_{k=1}^{p} r_{s_k} e^{j(l-1)(\alpha_k - \beta_k)} + \sigma^2\delta_{l,1} \\ &= \boldsymbol{r}_s^T\boldsymbol{b}_{l-1}(\omega) + \sigma^2\delta_{l,1}\end{aligned} \tag{54}$$

where $\boldsymbol{r}_s \triangleq [r_{s_1}, r_{s_2}, \cdots, r_{s_p}]^T$, $\boldsymbol{b}_k(\omega) \triangleq [e^{jk\omega_1}, e^{jk\omega_2}, \cdots, e^{jk\omega_p}]^T$, and $\omega_k \triangleq \alpha_k - \beta_k$. Obviously the corresponding relationship between the azimuth and elevation angles ϕ_k and θ_k are emerged into the "signals" $\{\tilde{r}_{ll}\}$, which are the correlations between the array data received by two ULAs, where $\tilde{r}_{11}$ is the autocorrelation of $z_0(n)$, while the others are cross-correlations between $x_l(n)$ and $z_l(n)$ for $l = 1, 2, \cdots, M-1$. Moreover $\{\tilde{r}_{ll}\}$ can be interpreted as the received "signals" for a ULA of M sensors illuminated by p "signals" $\{r_{s_k}\}$ with the "electrical angles" $\{\omega_k\}$.

Then from (54), by some simple algebraic manipulations, we can form the following $M \times M$ Toeplitz matrix with the "signals" $\{\tilde{r}_{ll}\}$ in (54)

$$\bar{\boldsymbol{R}}_{cc} \triangleq \mathrm{Toeplitz}(\tilde{\boldsymbol{r}}, \tilde{\boldsymbol{r}}^H) = \boldsymbol{A}(\omega)\bar{\boldsymbol{R}}_s\boldsymbol{A}^H(\omega) + \sigma^2\bar{\boldsymbol{I}}_M \tag{55}$$

where $\mathrm{Toeplitz}(\boldsymbol{c}, \boldsymbol{r}^H)$ denotes the Toeplitz operation which returns a nonsymmetric Toeplitz matrix having $\boldsymbol{c}$ as its first column and $\boldsymbol{r}^H$ as its first row, $\tilde{\boldsymbol{r}} \triangleq [\tilde{r}_{11}, \tilde{r}_{22}, \cdots, \tilde{r}_{MM}]^T$, and $\boldsymbol{A}(\omega) \triangleq [\boldsymbol{b}_0(\omega), \boldsymbol{b}_1(\omega), \cdots, \boldsymbol{b}_{M-1}(\omega)]^T$. Evidently we can find "electrical angles" $\{\omega_k\}$ by employing the OPM [9] on (55).

Thus by comparing the estimates $\{\hat{\omega}_k\}$ obtained from (55) with p^2 combinations of $\left\{(2\pi d/\lambda)(\cos\hat{\theta}_i - \cos\hat{\phi}_j)\right\}$ for $i, j = 1, 2, \cdots, p$, the pairs of $\{\hat{\theta}_i, \hat{\phi}_j\}$ can be matched, where the estimated elevation angle $\hat{\theta}_k$ and azimuth angle $\hat{\phi}_k$ are obtained separately by using the high-resolution direction estimation methods such as the ESPRIT [32] (see [4] for details).

Remark 4: As shown in (54) and (55), the estimation of parameter ω_k and hence the pair-matching of estimated azimuth and elevation angles are affected the additive noise and the difference between the parameters $\{\omega_k\}$ (i.e., $\{\cos\theta_k - \cos\phi_k\}$). Thus the performance of pair-matching may degrade when the SNR is low and/or the "virtual electrical angles" $\{\omega_k\}$ are spatially close. □

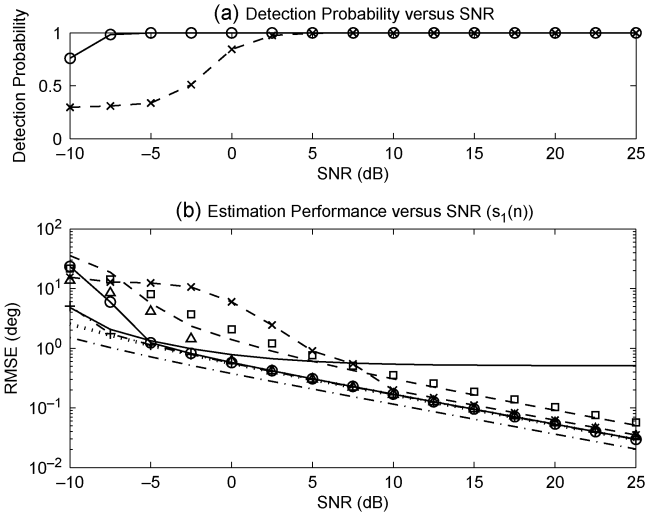

Fig. 2. (a) Detection probability. (b) RMSE of $s_1(n)$ versus the SNR for two uncorrelated signals (dash-dotted line with "+": root-MUSIC with correct pairing; "△": OPM with correct pairing; "□": SUMWE with correct pairing; solid line: JSVD; dashed line: MPM with correct pairing; dashed line with "x": CCM-ESPRIT; solid line with "o": proposed method; dotted line: theoretical RMSE of proposed method; and dash-dotted line: CRB) in Example 1 ($N = 100$, $M = 7$, $[\theta_1, \phi_1] = [45°, 65°]$, and $[\theta_2, \phi_2] = [75°, 80°]$).

4) Example 1—Performance Versus SNR: Now we examine the performance of the proposed method with respect to the SNR. Two uncorrelated signals impinge on the array along the elevation and azimuth angles $[\theta_1, \phi_1] = [45°, 65°]$ and $[\theta_2, \phi_2] = [75°, 80°]$ with the equal power, and the SNRs are varied from -10 to 25 dB, while the number of snapshots is $N = 100$.

In order to measure the overall performance of estimating the elevation and azimuth angles, we define a root-MSE (RMSE) of the kth incident signal $s_k(n)$ as

$$\mathrm{RMSE} \triangleq \sqrt{\frac{1}{\bar{N}}\sum_{i=1}^{\bar{N}}\left(\left(\theta_k - \hat{\theta}_k^{(i)}\right)^2 + \left(\phi_k - \hat{\phi}_k^{(i)}\right)^2\right)} \tag{56}$$

where $\bar{N}$ is the number of independent trials. The detection probability of successful pair-matching of the proposed CODE method is shown and compared with the CCM-ESPRIT [4] in Fig. 2(a), where the 1-D ESPRIT method [32] is used to estimate the azimuth and elevation angles independently in the latter, while the empirical RMSE of $s_1(n)$ is depicted in Fig. 2(b), where the theoretical RMSE obtained from (30) and (31), the stochastic Cramer-Rao lower bound (CRB) [6], [39], and the results of the CCM-ESPRIT [4], the JSVD [5], and the others with correct pairing [3], [9], [10] and [43], [47] are also plotted for comparison.

As mentioned in Remark 4, in spite of good estimation of the elevation and azimuth angles with the ESPRIT, the estimation error of the "virtual electrical angles" $\{\omega_k\}$ (i.e.,

$\{\cos\theta_k - \cos\phi_k\}$) causes the CCM-ESPRIT [4] to have unsuccessful pair-matching and worse DOA estimation at low to moderate SNRs in this empirical scenario as plotted in Fig. 2(a) and (b). On the other hand, as discussed in Remarks 1–3 and shown in Fig. 2(b), although the eigendecomposition is used in the MPM [3] and JSVD [5], the former with correct pairing [3] gives the estimate of elevation or azimuth angle with larger RMSE regardless of SNR owing to the biased estimate $\hat{\hat{\boldsymbol{P}}}$ in (43), and the latter [5] has larger RMSE at high SNR due to the inaccurate estimate $\hat{\phi}_k$ caused by the finite number of snapshots, while the SUMWE [10] performs worse because of the reduced working array aperture, and the OPM [9] has larger RMSE at low SNR as a result of the influence of additive noises, where the correct pair-matching is imposed on the results of these methods.

However, because the impact of additive noises is mitigated and the array data received by two ULAs are utilized more effectively and efficiently as shown in (6) and (16) [i.e., (28) and (29)], the proposed CODE method uses the cross-correlation matrix $\boldsymbol{R}_{xz}$ in (3) between two ULAs and its variants $\boldsymbol{J}_M\boldsymbol{R}_{xz}^*$, $\boldsymbol{R}_{xz}^H$, and $\boldsymbol{J}_M\boldsymbol{R}_{xz}^T$ to estimate the azimuth and elevation angles separately, and it generally performs better than the 2-D DOA estimation methods developed for the L-shaped array in the $x-z$ plane such as the MPM with correct pairing [3] and the JSVD [5] and the ordinary subspace-based methods such as the OPM [9] and the SUMWE [10] as plotted in Fig. 2(b), while it has similar performance to the root-MUSIC with correct pairing [43], [44], [47] at moderate and high SNRs, where the computationally burdensome eigendecomposition is also avoided in the CODE method. We note that the root-MUSIC and the JSVD provide relatively better estimate at very low SNR due to the noise suppression with eigendecomposition and correct pair-matching. Further the empirical RMSE of the proposed method for $s_1(n)$ is very close to the theoretical one given by (30) and (31) (except at very low SNR, and their difference is almost indistinguishable), and the difference between the theoretical RMSE and the CRB is small. Additionally, as demonstrated in Fig. 2(a), we can see that the proposed CODE method outperforms the CCM-ESPRIT [4] in pair-matching at low SNR. The results for $s_2(n)$ are similar and are omitted here.

5) Example 2—Performance Versus Number of Snapshots: Then we test the performance of the proposed method in terms of the number of snapshots. The number of snapshots is varied from 10 to 1000, and $\mathrm{SNR} = 0$ dB, while the other simulation parameters are the same with those in Example 1.

As shown in Fig. 3(a) and 3(b), even when the number of snapshots is rather small, the proposed CODE method generally outperforms the JSVD with automatic pairing [5], the CCM-ESPRIT [4], and the MPM with correct pairing [3], and it also performs well than the ordinary 1-D methods such as the OPM [9] and the SUMWE [10] with correct pairing, because of the good use of the cross-correlations and working array aperture. The root-MUSIC [43], [44], [47] performs better than the other methods due to the use of EVD and correct pairing as described in Example 1. Furthermore we also find that the empirical RMSE agrees very well with the theoretical one derived for larger number of snapshots in Section IV (except for a small number of snapshots).

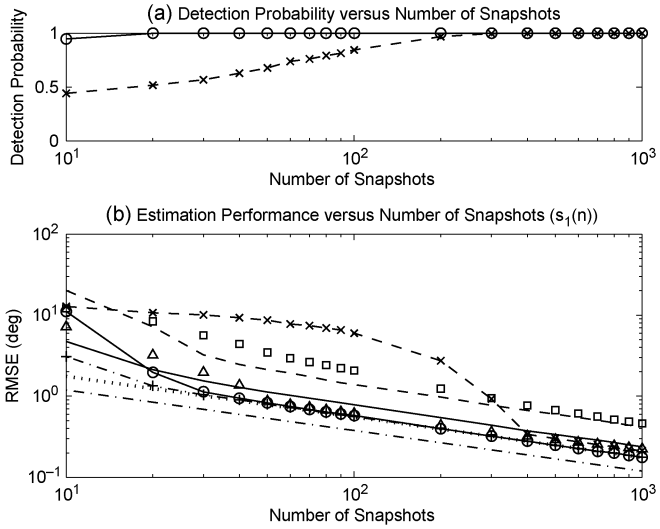

Fig. 3. (a) Detection probability. (b) RMSE of $s_1(n)$ versus the number of snapshots for two uncorrelated signals (dash-dotted line with "+": root-MUSIC with correct pairing; "△": OPM with correct pairing; "□": SUMWE with correct pairing; solid line: JSVD; dashed line: MPM with correct pairing; dashed line with "x": CCM-ESPRIT; solid line with "∘": proposed method; dotted line: theoretical RMSE of proposed method; and dash-dotted line: CRB) in Example 2 ($\mathrm{SNR} = 0$ dB, $M = 7$, $[\theta_1, \phi_1] = [45^\circ, 65^\circ]$, and $[\theta_2, \phi_2] = [75^\circ, 80^\circ]$).

6) Example 3—Performance Versus Correlation Factor: Here we evaluate the performance of the proposed method against the correlation between the incident signals. The signal $s_2(n)$ is a superposition of two uncorrelated signals $s_1(n)$ and $s_{2o}(n)$ with equal power given by

$$s_2(n) = \rho s_1(n) + \sqrt{1 - |\rho|^2}\, s_{2o}(n) \tag{57}$$

where the magnitude of the correlation factor ρ is varied between 0 and 0.9. The other parameters for simulation are similar to those in Example 1, except that $\mathrm{SNR} = 0$ dB.

As shown in Fig. 4(a) and (b), the proposed CODE method outperforms the CCM-ESPRIT [4] in pair-matching, and it is generally superior to the other methods such as the JSVD with automatic pairing [5], the CCM-ESPRIT [4], and the MPM with correct pairing [3], the OPM with correct pairing [9] and the SUMWE with correct pairing [10] in DOA estimation for uncorrelated and weakly correlated signals, but its estimation performance degrades significantly with the increasing correlation factor between the incident signals, because the decorrelation preprocessing is not employed. We also see that the root-MUSIC [43], [44], [47] has good estimation performance at low and relative high correlation factor because of the use of EVD and correct pairing, while the SUMWE tends to perform well for high correlated signals because of the subarray averaging.

7) Example 4—Performance Versus Angular Separation: Finally we assess the performance of the proposed method against the angular separation between two incident signals. In this example, three cases are considered, where the azimuth and elevation angles of the signal $s_2(n)$ are set to: 1) $\phi_2 = \phi_1 + \Delta\phi$ and $\theta_2 = 75^\circ$; 2) $\phi_2 = 80^\circ$ and $\theta_2 = \theta_1 + \Delta\theta$, and (3) $\phi_2 = \phi_1 + \Delta\phi$ and $\theta_2 = \theta_1 + \Delta\theta$ with $\Delta\phi = \Delta$, $\Delta\theta = 2\Delta$, and Δ is varied from 1° to 16°, while the other simulation parameters are the

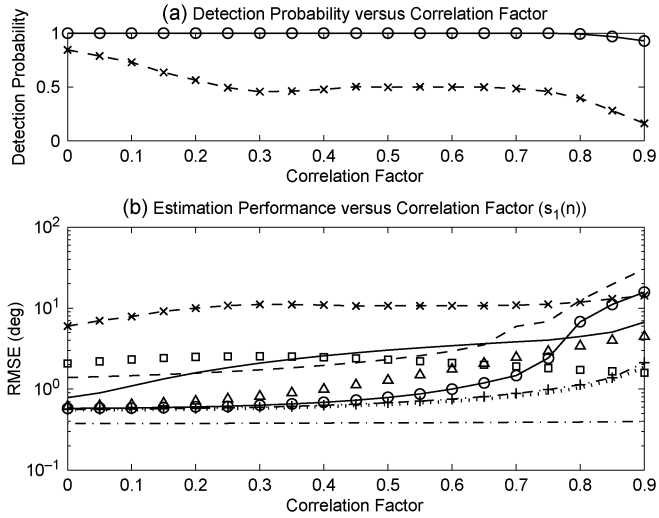

Fig. 4. (a) Detection probability. (b) RMSE of $s_1(n)$ versus the correlation factor of two signals (dash-dotted line with "+": root-MUSIC with correct pairing; "△": OPM with correct pairing; "□": SUMWE with correct pairing; solid line: JSVD; dashed line: MPM with correct pairing;dashed line with "x": CCM-ESPRIT; solid line with "∘": proposed method; dotted line: theoretical RMSE of proposed method; and dash-dotted line: CRB) in Example 3 ($\mathrm{SNR} = 0$ dB, $N = 100$, $M = 7$, $[\theta_1, \phi_1] = [45°, 65°]$, and $[\theta_2, \phi_2] = [75°, 80°]$).

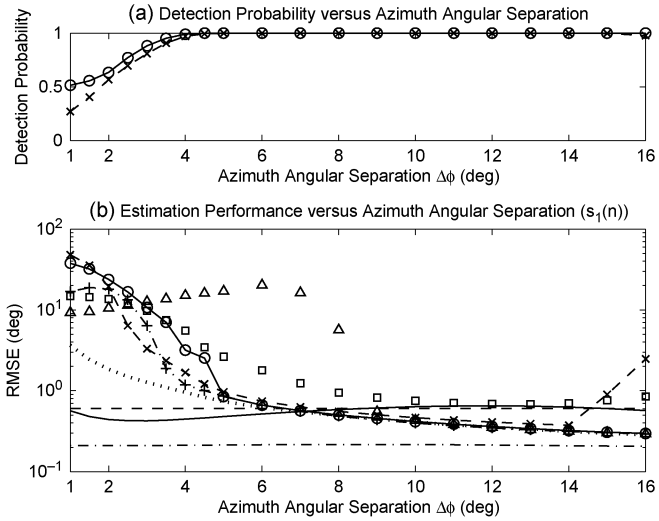

Fig. 5. (a) Detection probability. (b) RMSE of $s_1(n)$ versus the azimuth angular separation between two signals (dash-dotted line with "+": root-MUSIC with correct pairing; "△": OPM with correct pairing; "□": SUMWE with correct pairing; solid line: JSVD; dashed line: MPM with correct pairing; dashed line with "x": CCM-ESPRIT; solid line with "∘": proposed method; dotted line: theoretical RMSE of proposed method; and dash-dotted line: CRB) in Example 4 ($\mathrm{SNR} = 5$ dB, $N = 100$, $M = 7$, $[\theta_1, \phi_1] = [45°, 65°]$, and $[\theta_2, \phi_2] = [75°, \phi_1 + \Delta\phi]$).

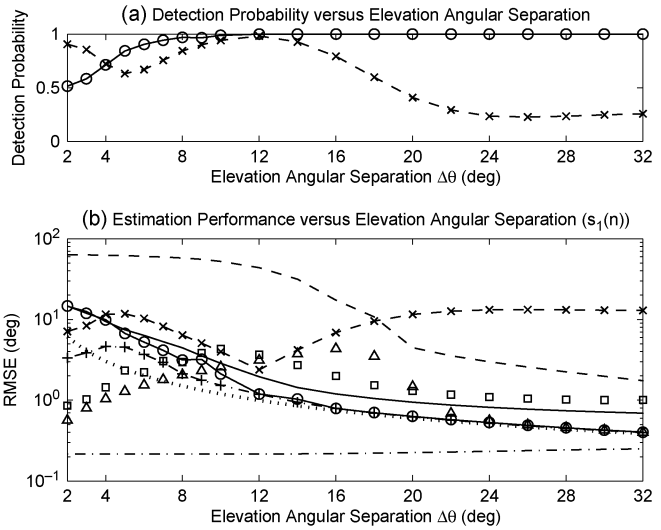

Fig. 6. (a) Detection probability. (b) RMSE of $s_1(n)$ versus the elevation angular separation between two signals (dash-dotted line with "+": root-MUSIC with correct pairing; "△": OPM with correct pairing; "□": SUMWE with correct pairing; solid line: JSVD; dashed line: MPM with correct pairing; dashed line with "x": CCM-ESPRIT; solid line with "∘": proposed method; dotted line: theoretical RMSE of proposed method; and dash-dotted line: CRB) in Example 4 ($\mathrm{SNR} = 5$ dB, $N = 100$, $M = 7$, $[\theta_1, \phi_1] = [45°, 65°]$, and $[\theta_2, \phi_2] = [\theta_1 + \Delta\theta, 80°]$).

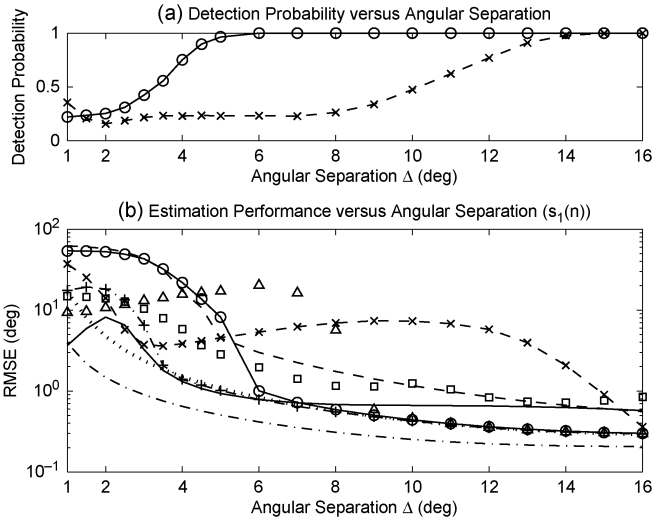

Fig. 7. (a) Detection probability. (b) RMSE of $s_1(n)$ versus the azimuth and elevation angular separation between two signals (dash-dotted line with "+": root-MUSIC with correct pairing; "△": OPM with correct pairing; "□": SUMWE with correct pairing; solid line: JSVD; dashed line: MPM with correct pairing; dashed line with "x": CCM-ESPRIT; solid line with "∘": proposed method; dotted line: theoretical RMSE of proposed method; and dash-dotted line: CRB) in Example 4 ($\mathrm{SNR} = 5$ dB, $N = 100$, $M = 7$, $[\theta_1, \phi_1] = [45°, 65°]$, and $[\theta_2, \phi_2] = [\theta_1 + \Delta\theta, \phi_1 + \Delta\phi]$).

same with those in Example 1, except that the SNR is fixed at $\mathrm{SNR} = 5$ dB.

The detection probabilities and the empirical RMSEs of $s_1(n)$ in terms of the azimuth angle separation $\Delta\phi$, the elevation angle separation $\Delta\theta$ and the azimuth and elevation angle separation Δ for the aforementioned cases are plotted in Figs. 5, 6 and 7, respectively. As described above, the proposed CODE method uses the cross-correlations between the array data received by two ULAs along the x and z axes simultaneously to estimate the azimuth and elevation angles and to match the pair of estimated azimuth and elevation angles, consequently its performances of DOA estimation and pair-matching become worse, when the incident signals become closely spaced in two dimensions of azimuth and elevation angles [i.e., case (3)], where the ranks of both array response matrices $\boldsymbol{A}(\phi)$ and $\boldsymbol{A}(\theta)$ tend to collapse. However, the proposed method generally pairs the estimated azimuth and elevation angles well than the CCM-ESPRIT [4] for small angular separations

as shown in Figs. 5(a), 6(a), and 7(a), though the latter [4] provides the DOA estimates with smaller RMSEs for some relatively small angular separations as shown in Figs. 5(b), 6(b) and 7(b), because it employs the ESPRIT with EVD [32] to estimate the azimuth and elevation angles from the array data of only one ULA independently. Furthermore when the angular separation becomes large, the empirical RMSEs agree very well with the theoretical RMSEs derived in Section IV and are commensurate with the quality of pair-matching shown in Figs. 5(a), 6(a), and 7(a), while they are much closer to that of the root-MUSIC [43], [44], [47] with EVD and correct pairing and smaller than that of the other methods [3]–[5], [9], [10]. We also see that these methods [3]–[5], [9], [10], [43], [47] provide DOA estimates with smaller RMSEs for some small angular separations because of the use of eigendecomposition in the root-MUSIC with correct pairing [43], [47], the MPM with correct pairing [3] and the JSVD [5] or due to the independent estimation of the azimuth and elevation angles from the array data from only one ULA in the OPM with correct pairing [9] and the SUMWE with correct pairing [10].

VI. Conclusion

A new computationally efficient subspace-based CODE method without eigendecomposition was proposed for 2-D DOA estimation of noncoherent signals impinging on the L-shaped sensor array, and the explicit expressions of asymptotic MSE of the estimated elevation and azimuth angles were derived. The simulation results showed that the proposed CODE method has less computational burden and superior estimation performance with high probability of successful pair-matching with a small number of snapshots and at low SNR and the theoretical analyzes agree well with empirical results.

Appendix A
Proof of Lemma

First, we examine the statistical performance of the estimate $\hat{\boldsymbol{P}}$ in (13). By dividing $\boldsymbol{x}(n)$ in (2) and $\bar{\boldsymbol{x}}(n)$ in (4) into two parts as $\boldsymbol{x}(n) = [\boldsymbol{x}_1^T(n), \boldsymbol{x}_2^T(n)]^T$, and $\bar{\boldsymbol{x}}(n) = [\bar{\boldsymbol{x}}_1^T(n), \bar{\boldsymbol{x}}_2^T(n)]^T$, where $\boldsymbol{x}_1(n) \triangleq [x_1(n), x_2(n), \cdots, x_p(n)]^T$, $\boldsymbol{x}_2(n) \triangleq [x_{p+1}(n), x_{p+2}(n), \cdots, x_M(n)]^T$, $\bar{\boldsymbol{x}}_1(n) \triangleq [x_M(n), x_{M-1}(n), \cdots, x_{M-p+1}(n)]^H$, and $\bar{\boldsymbol{x}}_2(n) \triangleq [x_{M-p}(n), x_{M-p-1}(n), \cdots, x_1(n)]^H$, from (3), (5), (6), (9), and (27), we have

$$\hat{\boldsymbol{R}}_{x1}\hat{\boldsymbol{R}}_{x1}^H = \hat{\boldsymbol{R}}_{xz1}\hat{\boldsymbol{R}}_{xz1}^H + \hat{\bar{\boldsymbol{R}}}_{xz1}\hat{\bar{\boldsymbol{R}}}_{xz1}^H \tag{A1}$$

$$\hat{\boldsymbol{R}}_{x1}\hat{\boldsymbol{R}}_{x2}^H = \hat{\boldsymbol{R}}_{xz1}\hat{\boldsymbol{R}}_{xz2}^H + \hat{\bar{\boldsymbol{R}}}_{xz1}\hat{\bar{\boldsymbol{R}}}_{xz2}^H \tag{A2}$$

where

$$\hat{\boldsymbol{R}}_{xz1} = \frac{1}{N}\sum_{n=1}^{N}\boldsymbol{x}_1(n)\boldsymbol{z}^H(n) \tag{A3}$$

$$\hat{\boldsymbol{R}}_{xz2} = \frac{1}{N}\sum_{n=1}^{N}\boldsymbol{x}_2(n)\boldsymbol{z}^H(n) \tag{A4}$$

$$\hat{\bar{\boldsymbol{R}}}_{xz1} = \frac{1}{N}\sum_{n=1}^{N}\bar{\boldsymbol{x}}_1(n)\boldsymbol{z}^T(n) \tag{A5}$$

$$\hat{\bar{\boldsymbol{R}}}_{xz2} = \frac{1}{N}\sum_{n=1}^{N}\bar{\boldsymbol{x}}_2(n)\boldsymbol{z}^T(n). \tag{A6}$$

Then by using the well-known formula for the expectation of four Gaussian random vectors with zero-mean and compatible dimensions (e.g., [38])

$$E\{\boldsymbol{a}\boldsymbol{b}^T\boldsymbol{c}\boldsymbol{d}^T\} = E\{\boldsymbol{a}\boldsymbol{b}^T\}E\{\boldsymbol{c}\boldsymbol{d}^T\} + \sum_{k=1}^{q}E\{c_k\boldsymbol{a}\}E\{b_k\boldsymbol{d}^T\} + E\left\{\boldsymbol{a}E\{\boldsymbol{b}^T\boldsymbol{c}\}\boldsymbol{d}^T\right\}$$

where $\boldsymbol{b} = [b_1, b_2, \cdots, b_q]^T$ and $\boldsymbol{c} = [c_1, c_2, \cdots, c_q]^T$, and by performing some straightforward manipulations under the basic assumptions on the data model, we can get

$$\begin{aligned}
&E\left\{\hat{\boldsymbol{R}}_{xz1}\hat{\boldsymbol{R}}_{xz1}^H\right\} \\
&= \frac{1}{N^2}E\left\{\sum_{n=1}^{N}\sum_{t=1}^{N}\boldsymbol{x}_1(n)\boldsymbol{z}^H(n)\boldsymbol{z}(t)\boldsymbol{x}_1^H(t)\right\} \\
&= \frac{1}{N^2}\left\{\sum_{n=1}^{N}\sum_{t=1}^{N}E\left\{\boldsymbol{x}_1(n)\boldsymbol{z}^H(n)\right\}E\left\{\boldsymbol{z}(t)\boldsymbol{x}_1^H(t)\right\}\right. \\
&\qquad + \sum_{n=1}^{N}\sum_{t=1}^{N}\left(\sum_{k=1}^{M}E\left\{z_{k-1}(t)\boldsymbol{x}_1(n)\right\}\right. \\
&\qquad\qquad \left.\times E\left\{z_{k-1}^*(n)\boldsymbol{x}_1^H(t)\right\}\right) \\
&\qquad \left. + \sum_{n=1}^{N}\sum_{t=1}^{N}E\left\{\boldsymbol{x}_1(n)E\left\{\boldsymbol{z}^H(n)\boldsymbol{z}(t)\right\}\boldsymbol{x}_1^H(t)\right\}\right\} \\
&= \boldsymbol{R}_{xz1}\boldsymbol{R}_{xz1}^H + 0 + \frac{1}{N}\bar{r}_{zz}\boldsymbol{R}_{xx1}
\end{aligned} \tag{A7}$$

where

$$\begin{aligned}
\bar{r}_{zz} &\triangleq E\left\{\boldsymbol{z}^H(n)\boldsymbol{z}(n)\right\} \\
&= \sum_{k=0}^{M-1}\boldsymbol{b}_k^T(\theta)\boldsymbol{R}_s\boldsymbol{b}_k^*(\theta) + M\sigma^2
\end{aligned} \tag{A8}$$

with $\boldsymbol{b}_k(\theta) \triangleq [e^{jk\alpha_1}, e^{jk\alpha_2}, \cdots, e^{jk\alpha_p}]^T$, and $\boldsymbol{R}_{xx1} \triangleq E\{\boldsymbol{x}_1(n)\boldsymbol{x}_1^H(n)\} = \boldsymbol{A}_1(\phi)\boldsymbol{R}_s\boldsymbol{A}_1^H(\phi) + \sigma^2\boldsymbol{I}_p$. In a similar fashion, we easily obtain

$$E\left\{\hat{\bar{\boldsymbol{R}}}_{xz1}\hat{\bar{\boldsymbol{R}}}_{xz1}^H\right\} = \bar{\boldsymbol{R}}_{xz1}\bar{\boldsymbol{R}}_{xz1}^H + \frac{1}{N}\bar{r}_{zz}^*\bar{\boldsymbol{R}}_{xx1} \tag{A9}$$

$$E\left\{\hat{\boldsymbol{R}}_{xz1}\hat{\boldsymbol{R}}_{xz2}^H\right\} = \boldsymbol{R}_{xz1}\boldsymbol{R}_{xz2}^H + \frac{1}{N}\bar{r}_{zz}\boldsymbol{R}_{xx12} \tag{A10}$$

$$E\left\{\hat{\bar{\boldsymbol{R}}}_{xz1}\hat{\bar{\boldsymbol{R}}}_{xz2}^H\right\} = \bar{\boldsymbol{R}}_{xz1}\bar{\boldsymbol{R}}_{xz2}^H + \frac{1}{N}\bar{r}_{zz}^*\bar{\boldsymbol{R}}_{xx12} \tag{A11}$$

where $\boldsymbol{R}_{xx12} \triangleq E\{\boldsymbol{x}_1(n)\boldsymbol{x}_2^H(n)\} = \boldsymbol{A}_1(\phi)\boldsymbol{R}_s\boldsymbol{A}_2^H(\phi)$, $\bar{\boldsymbol{R}}_{xx1} \triangleq E\{\bar{\boldsymbol{x}}_1(n)\bar{\boldsymbol{x}}_1^H(n)\} = \bar{\boldsymbol{A}}_1(\phi)\boldsymbol{R}_s\bar{\boldsymbol{A}}_1^H(\phi) + \sigma^2\boldsymbol{I}_p$, and $\bar{\boldsymbol{R}}_{xx12} \triangleq E\{\bar{\boldsymbol{x}}_1(n)\bar{\boldsymbol{x}}_2^H(n)\} = \bar{\boldsymbol{A}}_1(\phi)\boldsymbol{R}_s\bar{\boldsymbol{A}}_2^H(\phi)$ with $\bar{\boldsymbol{A}}_1 \triangleq [\boldsymbol{b}_M(\phi), \boldsymbol{b}_{M-1}(\phi), \cdots, \boldsymbol{b}_{M-p+1}(\phi)]^H$, $\bar{\boldsymbol{A}}_2 \triangleq [\boldsymbol{b}_{M-p}(\phi), \boldsymbol{b}_{M-p-1}(\phi), \cdots, \boldsymbol{b}_1(\phi)]^H$, and $\boldsymbol{b}_k(\phi) \triangleq [e^{jk\beta_1}, e^{jk\beta_2}, \cdots, e^{jk\beta_p}]^T$.

Since the received signals $\{x_k(n)\}$ and $\{z_k(n)\}$ are temporally complex white Gaussian random processes under the model assumptions and $\hat{\boldsymbol{R}}_{x1}\hat{\boldsymbol{R}}_{x1}^H$ in (A1) is the time-average of the products $\boldsymbol{x}_1(n)\boldsymbol{z}^H(n)$ and $\bar{\boldsymbol{x}}_1(n)\boldsymbol{z}^T(n)$ for $1 \le n \le N$, we can see that $(\hat{\boldsymbol{R}}_{x1}\hat{\boldsymbol{R}}_{x1}^H)^{-1}$ in (13) tends to be "slowly" time-varying with respect to (w.r.t.) $\boldsymbol{x}_1(n)\boldsymbol{z}^H(n)$ and $\bar{\boldsymbol{x}}_1(n)\boldsymbol{z}^T(n)$ (i.e., $\hat{\boldsymbol{R}}_{xz1}$ and $\hat{\bar{\boldsymbol{R}}}_{xz1}$) and hence it is "almost" independent of $\boldsymbol{x}_1(n)\boldsymbol{z}^H(n)$ and $\bar{\boldsymbol{x}}_1(n)\boldsymbol{z}^T(n)$ (i.e., $\hat{\boldsymbol{R}}_{x1}\hat{\boldsymbol{R}}_{x1}^H$) (cf. [40]). Then following the fact $(\hat{\boldsymbol{R}}_{x1}\hat{\boldsymbol{R}}_{x1}^H)^{-1}\hat{\boldsymbol{R}}_{x1}\hat{\boldsymbol{R}}_{x1}^H = \boldsymbol{I}_p$ and by applying the averaging principle (e.g., [41] and [42]), we can obtain

$$\begin{aligned}\boldsymbol{I}_p &= E\left\{\left(\hat{\boldsymbol{R}}_{x1}\hat{\boldsymbol{R}}_{x1}^H\right)^{-1}\hat{\boldsymbol{R}}_{x1}\hat{\boldsymbol{R}}_{x1}^H\right\}\\ &\approx E\left\{\left(\hat{\boldsymbol{R}}_{x1}\hat{\boldsymbol{R}}_{x1}^H\right)^{-1}\right\}E\left\{\hat{\boldsymbol{R}}_{x1}\hat{\boldsymbol{R}}_{x1}^H\right\}. \qquad \text{(A12)}\end{aligned}$$

Hence from (A12), (A1), (A7), and (A9), we can approximate the expectation of the inverse matrix $(\hat{\boldsymbol{R}}_{x1}\hat{\boldsymbol{R}}_{x1}^H)^{-1}$ in (13) as

$$\begin{aligned}&E\left\{\left(\hat{\boldsymbol{R}}_{x1}\hat{\boldsymbol{R}}_{x1}^H\right)^{-1}\right\}\\ &\quad\approx\left(E\left\{\hat{\boldsymbol{R}}_{x1}\hat{\boldsymbol{R}}_{x1}^H\right\}\right)^{-1}\\ &\quad=\left(\bar{\boldsymbol{R}}_{x1}\boldsymbol{R}_{x1}^H+\frac{1}{N}\left(\bar{r}_{zz}\boldsymbol{R}_{xx1}+\bar{r}_{zz}^*\bar{\boldsymbol{R}}_{xx1}\right)\right)^{-1}. \qquad \text{(A13)}\end{aligned}$$

Similarly we can find that $(\hat{\boldsymbol{R}}_{x1}\hat{\boldsymbol{R}}_{x1}^H)^{-1}$ in (13) is "almost" independent of $\boldsymbol{x}_2(n)\boldsymbol{z}^H(n)$ and $\bar{\boldsymbol{x}}_2(n)\boldsymbol{z}^T(n)$ (i.e., $\hat{\boldsymbol{R}}_{x1}\hat{\boldsymbol{R}}_{x2}^H$ in (13)) (cf. [40]), from (A2), (A10)–(A13), and (13), and consequently we can get

$$\begin{aligned}E\{\hat{\boldsymbol{P}}_x\}&\approx E\left\{\left(\hat{\boldsymbol{R}}_{x1}\hat{\boldsymbol{R}}_{x1}^H\right)^{-1}\right\}E\left\{\hat{\boldsymbol{R}}_{x1}\hat{\boldsymbol{R}}_{x2}^H\right\}\\ &\approx\left(E\left\{\hat{\boldsymbol{R}}_{x1}\hat{\boldsymbol{R}}_{x1}^H\right\}\right)^{-1}E\left\{\hat{\boldsymbol{R}}_{x1}\hat{\boldsymbol{R}}_{x2}^H\right\}\\ &=\left(\boldsymbol{R}_{x1}\boldsymbol{R}_{x1}^H+\frac{1}{N}\left(\bar{r}_{zz}\boldsymbol{R}_{xx1}+\bar{r}_{zz}^*\bar{\boldsymbol{R}}_{xx1}\right)\right)^{-1}\\ &\quad\cdot\left(\boldsymbol{R}_{x1}\boldsymbol{R}_{x2}^H+\frac{1}{N}\left(\bar{r}_{zz}\boldsymbol{R}_{xx12}+\bar{r}_{zz}^*\bar{\boldsymbol{R}}_{xx12}\right)\right). \qquad \text{(A14)}\end{aligned}$$

Thus as the number of snapshots N tends to infinity, from (A14), we have

$$\lim_{N\to\infty}\hat{\boldsymbol{P}}_x = \boldsymbol{P}_x \qquad \text{(A15)}$$

i.e., the LS estimate $\hat{\boldsymbol{P}}_x$ in (13) is asymptotically consistent.

Therefore it follows from (A15) that the cost function $f(\phi)$ in (11) converges to the true cost function $f_o(\phi) \triangleq \bar{\boldsymbol{a}}^H(\phi)\boldsymbol{\Pi}_x\bar{\boldsymbol{a}}(\phi)$ w.p.1 and uniformly in ϕ when $N \to \infty$, where $\boldsymbol{\Pi}_x \triangleq \boldsymbol{Q}_x(\boldsymbol{Q}_x^H\boldsymbol{Q}_x)^{-1}\boldsymbol{Q}_x^H$, and the minima of $f_o(\theta)$ are achieved if and only if $\phi = \phi_k$. Thus the estimates $\{\hat{\phi}_k\}$ approach the true parameters $\{\phi_k\}$ w.p.1 as $N \to \infty$.

Furthermore the consistency of the estimate $\hat{\theta}$ can be established in a similar way, i.e., the estimates $\{\hat{\theta}_k\}$ approach the true parameters $\{\theta_k\}$ w.p.1 as $N \to \infty$. ■

APPENDIX B
PROOF OF THEOREM 1

Because the estimated azimuth angle $\hat{\phi}_k$ is obtained by minimizing the cost function $f(\phi)$ in (11) and it is a consistent estimate for a sufficiently large number of snapshots N, we can obtain the second-order approximation of the derivative of $f(\phi)$ about the true value ϕ_k as (cf. [10], [45], [46], and references therein)

$$0 = f'(\hat{\phi}_k) \approx f'(\phi_k) + f''(\phi_k)(\hat{\phi}_k - \phi_k) \qquad \text{(B1)}$$

where the second- and higher order terms in (B1) can be neglected, and the first- and second-order derivatives of $f(\phi)$ with respect to the scalar variable ϕ are given by

$$f'(\phi) \triangleq \frac{df(\phi)}{d\phi} = 2\mathrm{Re}\left\{\boldsymbol{d}^H(\phi)\hat{\boldsymbol{\Pi}}_x\boldsymbol{a}(\phi)\right\} \qquad \text{(B2)}$$

$$f''(\theta) \triangleq \frac{df'(\phi)}{d\phi} = 2\mathrm{Re}\left\{\tilde{\boldsymbol{d}}^H(\phi)\hat{\boldsymbol{\Pi}}_x\boldsymbol{a}(\phi) + \boldsymbol{d}^H(\phi)\hat{\boldsymbol{\Pi}}_x\boldsymbol{d}(\phi)\right\} \qquad \text{(B3)}$$

in which $\tilde{\boldsymbol{d}}(\phi) \triangleq d\boldsymbol{d}(\phi)/d\phi$. From (B1)–(B3), we can obtain by performing a length but straightforward derivation leads to the first-order expression for the estimation error $\Delta\phi_k \triangleq \hat{\phi}_k - \phi_k$ can be obtained as

$$\begin{aligned}\Delta\phi_k &\triangleq \hat{\phi}_k - \phi_k\\ &\approx -\frac{f'(\phi_k)}{f''(\phi_k)} \approx -\frac{\mathrm{Re}\left\{\boldsymbol{d}^H(\phi_k)\hat{\boldsymbol{\Pi}}_x\boldsymbol{a}(\phi_k)\right\}}{\boldsymbol{d}^H(\phi_k)\boldsymbol{\Pi}_x\boldsymbol{d}(\phi_k)} \qquad \text{(B4)}\end{aligned}$$

where the estimated orthogonal projector $\hat{\boldsymbol{\Pi}}_x$ in the denominator of (B4) (i.e. (B3)) can be replaced with the true one $\boldsymbol{\Pi}_x$ without affecting the asymptotic property of estimate $\hat{\phi}_k$ [10], [45], [46]. Furthermore the estimated orthogonal projector $\hat{\boldsymbol{\Pi}}_x$ in (B4) can be approximated as [10], [46]

$$\begin{aligned}\hat{\boldsymbol{\Pi}}_x &= \hat{\boldsymbol{Q}}_x\left(\hat{\boldsymbol{Q}}_x^H\hat{\boldsymbol{Q}}_x\right)^{-1}\hat{\boldsymbol{Q}}_x^H\\ &\approx \boldsymbol{Q}_x\left(\boldsymbol{Q}_x^H\boldsymbol{Q}_x\right)^{-1}\boldsymbol{Q}_x^H + (\hat{\boldsymbol{Q}}_x - \boldsymbol{Q}_x)\left(\boldsymbol{Q}_x^H\boldsymbol{Q}_x\right)^{-1}\boldsymbol{Q}_x^H\\ &\quad + \boldsymbol{Q}_x\left(\left(\hat{\boldsymbol{Q}}_x^H\hat{\boldsymbol{Q}}_x\right)^{-1}\hat{\boldsymbol{Q}}_x^H - \left(\boldsymbol{Q}_x^H\boldsymbol{Q}_x\right)^{-1}\boldsymbol{Q}_x^H\right)\\ &= (\hat{\boldsymbol{Q}}_x - \boldsymbol{Q}_x)\left(\boldsymbol{Q}_x^H\boldsymbol{Q}_x\right)^{-1}\boldsymbol{Q}_x^H + \boldsymbol{Q}_x\left(\hat{\boldsymbol{Q}}_x^H\hat{\boldsymbol{Q}}_x\right)^{-1}\hat{\boldsymbol{Q}}_x^H\\ &\approx (\hat{\boldsymbol{Q}}_x - \boldsymbol{Q}_x)\left(\boldsymbol{Q}_x^H\boldsymbol{Q}_x\right)^{-1}\boldsymbol{Q}_x^H + \boldsymbol{Q}_x\left(\boldsymbol{Q}_x^H\boldsymbol{Q}_x\right)^{-1}\\ &\quad\cdot(\hat{\boldsymbol{Q}}_x - \boldsymbol{Q}_x)^H + \boldsymbol{Q}_x\left(\hat{\boldsymbol{Q}}_x^H\hat{\boldsymbol{Q}}_x\right)^{-1}\boldsymbol{Q}_x^H. \qquad \text{(B5)}\end{aligned}$$

Then by substituting the approximation of $\hat{\boldsymbol{\Pi}}_x$ in (B5) into (B4) and using the fact that $\boldsymbol{Q}_x^H\boldsymbol{a}(\phi_k) = \boldsymbol{0}_{(M-p)\times 1}$, the estimation error $\Delta\phi_k$ in (B3) can be approximately given by

$$\begin{aligned}\Delta\phi_k &\approx -\frac{\mathrm{Re}\{\boldsymbol{d}^H(\phi_k)\boldsymbol{Q}_x\left(\boldsymbol{Q}_x^H\boldsymbol{Q}_x\right)^{-1}\hat{\boldsymbol{Q}}_x^H\boldsymbol{a}(\phi_k)\}}{\boldsymbol{d}^H(\phi_k)\boldsymbol{\Pi}_x\boldsymbol{d}(\phi_k)}\\ &= -\frac{\mathrm{Re}\{\mu_k\}}{H_{xkk}} \qquad \text{(B6)}\end{aligned}$$

where

$$\mu_k \triangleq \boldsymbol{d}^H(\phi_k)\boldsymbol{Q}_x\left(\boldsymbol{Q}_x^H\boldsymbol{Q}_x\right)^{-1}\hat{\boldsymbol{Q}}_x^H\boldsymbol{a}(\phi_k). \qquad \text{(B7)}$$

Consequently because the estimate $\hat{\phi}_k$ is consistent, from (B6), the MSE (or variance) of the estimation error $\Delta\phi_k$ is given by

$$\begin{aligned}\mathrm{MSE}(\hat{\phi}_k) &\triangleq E\left\{(\Delta\phi_k)^2\right\} = \mathrm{var}(\hat{\phi}_k) \\ &\approx \frac{1}{2H_{xkk}^2}\mathrm{Re}\left\{E\left\{\mu_k^2\right\} + E\left\{|\mu_k|^2\right\}\right\} \quad \text{(B8)}\end{aligned}$$

where the fact that $\mathrm{Re}\{\mu_i\}\mathrm{Re}\{\mu_k\} = 0.5(\mathrm{Re}\{\mu_i\mu_k\} + \mathrm{Re}\{\mu_i\mu_k^*\})$ is used implicitly.

By utilizing the partitions in (7) and (9), we can rewrite μ_k in (B7) as

$$\begin{aligned}\mu_k &\triangleq \boldsymbol{d}^H(\phi_k)\boldsymbol{Q}_x\left(\boldsymbol{Q}_x^H\boldsymbol{Q}_x\right)^{-1}\hat{\boldsymbol{Q}}_x^H\boldsymbol{a}(\phi_k) \\ &= \boldsymbol{d}^H(\phi_k)\boldsymbol{Q}_x\left(\boldsymbol{Q}_x^H\boldsymbol{Q}_x\right)^{-1}\tilde{\boldsymbol{P}}_x^H\boldsymbol{a}_1(\phi_k) \quad \text{(B9)}\end{aligned}$$

where

$$\begin{aligned}\tilde{\boldsymbol{P}}_x^H &\triangleq \hat{\boldsymbol{P}}_x^H - \boldsymbol{P}_x^H \\ &= \left(\hat{\boldsymbol{R}}_{x2}\hat{\boldsymbol{R}}_{x1}^H - \boldsymbol{P}_x^H\left(\hat{\boldsymbol{R}}_{x1}\hat{\boldsymbol{R}}_{x1}^H\right)\right)\left(\hat{\boldsymbol{R}}_{x1}\hat{\boldsymbol{R}}_{x1}^H\right)^{-1} \\ &= -\boldsymbol{Q}_x^H\hat{\boldsymbol{R}}_x\hat{\boldsymbol{R}}_{x1}^H\left(\hat{\boldsymbol{R}}_{x1}\hat{\boldsymbol{R}}_{x1}^H\right)^{-1} \\ &\approx -\boldsymbol{Q}_x^H\left(\boldsymbol{R}_x\left(\hat{\boldsymbol{R}}_{x1}^H - \boldsymbol{R}_{x1}^H\right) + \hat{\boldsymbol{R}}_x\boldsymbol{R}_{x1}^H\right)\left(\boldsymbol{R}_{x1}\boldsymbol{R}_{x1}^H\right)^{-1} \\ &= -\boldsymbol{Q}_x^H\hat{\boldsymbol{R}}_x\boldsymbol{R}_{x1}^H\left(\boldsymbol{R}_{x1}\boldsymbol{R}_{x1}^H\right)^{-1}. \quad \text{(B10)}\end{aligned}$$

By substituting the approximation of the matrix $\tilde{\boldsymbol{P}}_z^H$ in (B10) into μ_k in (B9) and from (9), (3), and (5), we can get

$$\begin{aligned}\mu_k &= -\boldsymbol{d}^H(\phi_k)\boldsymbol{\Pi}_x\hat{\boldsymbol{R}}_x\boldsymbol{R}_{x1}^H\left(\boldsymbol{R}_{x1}\boldsymbol{R}_{x1}^H\right)^{-1}\boldsymbol{a}_1(\phi_k) \\ &= -\boldsymbol{g}^H(\phi_k)[\hat{\boldsymbol{R}}_{xz}, \hat{\bar{\boldsymbol{R}}}_{xz}][\boldsymbol{R}_{xz1}, \bar{\boldsymbol{R}}_{xz1}]^H \\ &\quad \cdot\left(\boldsymbol{R}_{x1}\boldsymbol{R}_{x1}^H\right)^{-1}\boldsymbol{a}_1(\phi_k) \\ &= \mu_{k1} + \mu_{k2} \quad \text{(B11)}\end{aligned}$$

where

$$\begin{aligned}\mu_{k1} &\triangleq -\boldsymbol{g}^H(\phi_k)\hat{\boldsymbol{R}}_{xz}\boldsymbol{h}(\phi_k) \\ &= -\frac{1}{N}\sum_{n=1}^{N}\boldsymbol{g}^H(\phi_k)\boldsymbol{x}(n)\boldsymbol{z}^H(n)\boldsymbol{h}(\phi_k) \quad \text{(B12)} \\ \mu_{k2} &\triangleq -\boldsymbol{g}^H(\phi_k)\hat{\bar{\boldsymbol{R}}}_{xz}\bar{\boldsymbol{h}}(\phi_k) \\ &= -\frac{1}{N}\sum_{n=1}^{N}\boldsymbol{g}^H(\phi_k)\boldsymbol{J}_M\boldsymbol{x}^*(n)\boldsymbol{z}^T(n)\bar{\boldsymbol{h}}(\phi_k). \quad \text{(B13)}\end{aligned}$$

Then from (B11), the two terms of $\mathrm{MSE}(\hat{\phi}_k)$ in (B8) can be obtained as

$$\begin{aligned}E\left\{\mu_k^2\right\} &= E\left\{\mu_{k1}^2 + \mu_{k2}^2 + 2\mu_{k1}\mu_{k2}\right\} \quad \text{(B14)} \\ E\left\{|\mu_k|^2\right\} &= E\left\{|\mu_{k1}|^2 + \mu_{k1}\mu_{k2}^* \right. \\ &\qquad \left. + \mu_{k1}^*\mu_{k2} + |\mu_{k2}|^2\right\}. \quad \text{(B15)}\end{aligned}$$

Under the basic assumptions on the data model, and by using the well-known formula for the expectation of four Gaussian random variables with zero-mean (e.g., [38])

$$\begin{aligned}E\{x_1x_2x_3x_4\} &= E\{x_1x_2\}E\{x_3x_4\} \\ &\quad + E\{x_1x_3\}E\{x_2x_4\} + E\{x_1x_4\}E\{x_2x_3\}\end{aligned}$$

and considering the fact that $\boldsymbol{Q}_x$ spans the null space of $\boldsymbol{A}(\phi)$ (i.e., $\boldsymbol{Q}_x^H\boldsymbol{A}(\phi) = \boldsymbol{O}_{(M-p)\times p}$), from (3) and (5), we get

$$\begin{aligned}&E\left\{\mu_{k1}^2\right\} \\ &= \frac{1}{N^2}E\left\{\sum_{n=1}^{N}\sum_{t=1}^{N}\boldsymbol{g}^H(\phi_k)\boldsymbol{x}(n)\boldsymbol{z}^H(n)\boldsymbol{h}(\phi_k)\right. \\ &\qquad \left.\cdot\,\boldsymbol{g}^H(\phi_k)\boldsymbol{x}(t)\boldsymbol{z}^H(t)\boldsymbol{h}(\phi_k)\right\} \\ &= \frac{1}{N^2}\sum_{n=1}^{N}\sum_{t=1}^{N}\left\{E\left\{\boldsymbol{g}^H(\phi_k)\boldsymbol{x}(n)\boldsymbol{z}^H(n)\boldsymbol{h}(\phi_k)\right\}\right. \\ &\qquad \cdot E\left\{\boldsymbol{g}^H(\phi_k)\boldsymbol{x}(t)\boldsymbol{z}^H(t)\boldsymbol{h}(\phi_k)\right\} \\ &\qquad + E\left\{\boldsymbol{g}^H(\phi_k)\boldsymbol{x}(n)\boldsymbol{x}^T(t)\boldsymbol{g}^*(\phi_k)\right\} \\ &\qquad \cdot E\left\{\boldsymbol{h}^T(\phi_k)\boldsymbol{z}^*(n)\boldsymbol{z}^H(t)\boldsymbol{h}(\phi_k)\right\} \\ &\qquad + E\left\{\boldsymbol{g}^H(\phi_k)\boldsymbol{x}(n)\boldsymbol{z}^H(t)\boldsymbol{h}(\phi_k)\right\} \\ &\qquad \left.\cdot E\left\{\boldsymbol{g}^H(\phi_k)\boldsymbol{x}(t)\boldsymbol{z}^H(n)\boldsymbol{h}(\phi_k)\right\}\right\} \\ &= \boldsymbol{g}^H(\phi_k)\boldsymbol{R}_{xz}\boldsymbol{h}(\phi_k)\boldsymbol{g}^H(\phi_k)\boldsymbol{R}_{xz}\boldsymbol{h}(\phi_k) + 0 \\ &\quad + \frac{1}{N}\boldsymbol{g}^H(\phi_k)\bar{\boldsymbol{R}}_{xz}\boldsymbol{h}(\phi_k)\boldsymbol{g}^H(\phi_k)\bar{\boldsymbol{R}}_{xz}\boldsymbol{h}(\phi_k) = 0 \quad \text{(B16)} \\ &E\left\{\mu_{k2}^2\right\} \\ &= \frac{1}{N^2}E\left\{\sum_{n=1}^{N}\sum_{t=1}^{N}\boldsymbol{g}^H(\phi_k)\boldsymbol{J}_M\boldsymbol{x}^*(n)\boldsymbol{z}^T(n)\bar{\boldsymbol{h}}(\phi_k)\right. \\ &\qquad \left.\cdot\,\boldsymbol{g}^H(\phi_k)\boldsymbol{J}_M\boldsymbol{x}^*(t)\boldsymbol{z}^T(t)\bar{\boldsymbol{h}}(\phi_k)\right\} \\ &= \frac{1}{N^2}\sum_{n=1}^{N}\sum_{t=1}^{N}\left\{E\left\{\boldsymbol{g}^H(\phi_k)\boldsymbol{J}_M\boldsymbol{x}^*(n)\boldsymbol{z}^T(n)\bar{\boldsymbol{h}}(\phi_k)\right\}\right. \\ &\qquad \cdot E\left\{\boldsymbol{g}^H(\phi_k)\boldsymbol{J}_M\boldsymbol{x}^*(t)\boldsymbol{z}^T(t)\bar{\boldsymbol{h}}(\phi_k)\right\} \\ &\qquad + E\left\{\boldsymbol{g}^H(\phi_k)\boldsymbol{J}_M\boldsymbol{x}^*(n)\boldsymbol{x}^H(t)\boldsymbol{J}_M\boldsymbol{g}^*(\phi_k)\right\} \\ &\qquad \cdot E\left\{\bar{\boldsymbol{h}}^T(\phi_k)\boldsymbol{z}(n)\boldsymbol{z}^T(t)\bar{\boldsymbol{h}}(\phi_k)\right\} \\ &\qquad + E\left\{\boldsymbol{g}^H(\phi_k)\boldsymbol{J}_M\boldsymbol{x}^*(n)\boldsymbol{z}^T(t)\bar{\boldsymbol{h}}(\phi_k)\right\} \\ &\qquad \left.\cdot E\left\{\boldsymbol{g}^H(\phi_k)\boldsymbol{J}_M\boldsymbol{x}^*(t)\boldsymbol{z}^T(n)\bar{\boldsymbol{h}}(\phi_k)\right\}\right\} \\ &= \boldsymbol{g}^H(\phi_k)\bar{\boldsymbol{R}}_{xz}\bar{\boldsymbol{h}}(\phi_k)\boldsymbol{g}^H(\phi_k)\bar{\boldsymbol{R}}_{xz}\bar{\boldsymbol{h}}(\phi_k) + 0 \\ &\quad + \frac{1}{N}\boldsymbol{g}^H(\phi_k)\bar{\boldsymbol{R}}_{xz}\bar{\boldsymbol{h}}(\phi_k)\boldsymbol{g}^H(\phi_k)\bar{\boldsymbol{R}}_{xz}\bar{\boldsymbol{h}}(\phi_k) = 0 \quad \text{(B17)} \\ &E\{\mu_{k1}\mu_{k2}\} \\ &= \frac{1}{N^2}E\left\{\sum_{n=1}^{N}\sum_{t=1}^{N}\boldsymbol{g}^H(\phi_k)\boldsymbol{x}(n)\boldsymbol{z}^H(n)\boldsymbol{h}(\phi_k)\right. \\ &\qquad \left.\cdot\,\boldsymbol{g}^H(\phi_k)\boldsymbol{J}_M\boldsymbol{x}^*(t)\boldsymbol{z}^T(t)\bar{\boldsymbol{b}}(\phi_k)\right\} \\ &= \frac{1}{N^2}\sum_{n=1}^{N}\sum_{t=1}^{N}\left\{E\left\{\boldsymbol{g}^H(\phi_k)\boldsymbol{x}(n)\boldsymbol{z}^H(n)\boldsymbol{h}(\phi_k)\right\}\right. \\ &\qquad \cdot E\left\{\boldsymbol{g}^H(\phi_k)\boldsymbol{J}_M\boldsymbol{x}^*(t)\boldsymbol{z}^T(t)\bar{\boldsymbol{h}}(\phi_k)\right\} \\ &\qquad + E\left\{\boldsymbol{g}^H(\phi_k)\boldsymbol{x}(n)\boldsymbol{x}^H(t)\boldsymbol{J}_M\boldsymbol{g}^*(\phi_k)\right\} \\ &\qquad \cdot E\left\{\bar{\boldsymbol{h}}^T(\phi_k)\boldsymbol{z}(t)\boldsymbol{z}^H(n)\boldsymbol{h}(\phi_k)\right\} \\ &\qquad + E\left\{\boldsymbol{g}^H(\phi_k)\boldsymbol{x}(n)\boldsymbol{z}^T(t)\bar{\boldsymbol{h}}(\phi_k)\right\} \\ &\qquad \left.\cdot E\left\{\boldsymbol{g}^H(\phi_k)\boldsymbol{J}_M\boldsymbol{x}^*(t)\boldsymbol{z}^H(n)\boldsymbol{h}(\phi_k)\right\}\right\}\end{aligned}$$

$$
\begin{aligned}
&= \boldsymbol{g}^H(\phi_k)\boldsymbol{R}_{xz}\boldsymbol{h}(\phi_k)\boldsymbol{g}^H(\phi_k)\bar{\boldsymbol{R}}_{xz}\bar{\boldsymbol{h}}(\phi_k) \\
&\quad + \frac{1}{N}\boldsymbol{g}^H(\phi_k)\boldsymbol{R}_{xx}\boldsymbol{J}_M\boldsymbol{g}^*(\phi_k)\bar{\boldsymbol{h}}^T(\phi_k)\boldsymbol{R}_{zz}\boldsymbol{h}(\phi_k) + 0 \\
&= \frac{1}{N}\boldsymbol{g}^H(\phi_k)(\boldsymbol{A}(\phi)\boldsymbol{R}_s\boldsymbol{A}^H(\phi) + \sigma^2\boldsymbol{I}_M)\boldsymbol{J}_M \\
&\quad \cdot \boldsymbol{g}^*(\phi_k)\bar{\boldsymbol{h}}^T(\phi_k)\bar{\boldsymbol{R}}_{zz}\boldsymbol{h}(\phi_k) \\
&= \frac{1}{N}\sigma^2\boldsymbol{g}^H(\phi_k)\boldsymbol{J}_M\boldsymbol{g}^*(\phi_k)\bar{\boldsymbol{h}}^T(\phi_k)\bar{\boldsymbol{R}}_{zz}\boldsymbol{h}(\phi_k) \qquad \text{(B18)}
\end{aligned}
$$

$$
\begin{aligned}
&E\{|\mu_{k1}|^2\} \\
&= \frac{1}{N^2}E\Bigg\{\sum_{n=1}^{N}\sum_{t=1}^{N}\boldsymbol{g}^H(\phi_k)\boldsymbol{x}(n)\boldsymbol{z}^H(n)\boldsymbol{h}(\phi_k)\boldsymbol{g}^T(\phi_k)\boldsymbol{x}^*(t) \\
&\qquad \cdot \boldsymbol{z}^T(t)\boldsymbol{h}^*(\phi_k)\Bigg\} \\
&= \frac{1}{N^2}\sum_{n=1}^{N}\sum_{t=1}^{N}\{E\{\boldsymbol{g}^H(\phi_k)\boldsymbol{x}(n)\boldsymbol{z}^H(n)\boldsymbol{h}(\phi_k)\} \\
&\qquad \cdot E\{\boldsymbol{g}^T(\phi_k)\boldsymbol{x}^*(t)\boldsymbol{z}^T(t)\boldsymbol{h}^*(\phi_k)\} \\
&\qquad + E\{\boldsymbol{g}^H(\phi_k)\boldsymbol{x}(n)\boldsymbol{x}^H(t)\boldsymbol{g}(\phi_k)\} \\
&\qquad \cdot E\Big\{\boldsymbol{h}^H(\phi_k)\boldsymbol{z}(t)\boldsymbol{z}^H(n)\boldsymbol{h}(\phi_k)\Big\} \\
&\qquad + E\{\boldsymbol{g}^H(\phi_k)\boldsymbol{x}(n)\boldsymbol{z}^T(t)\boldsymbol{h}^*(\phi_k)\} \\
&\qquad \cdot E\{\boldsymbol{g}^T(\phi_k)\boldsymbol{x}^*(t)\boldsymbol{z}^H(n)\boldsymbol{h}(\phi_k)\}\} \\
&= \boldsymbol{g}^H(\phi_k)\boldsymbol{R}_{xz}\boldsymbol{h}(\phi_k)\boldsymbol{g}^T(\phi_k)\boldsymbol{R}_{xz}^*\boldsymbol{h}^*(\phi_k) \\
&\quad + \frac{1}{N}\boldsymbol{g}^H(\phi_k)\boldsymbol{R}_{xx}\boldsymbol{g}(\phi_k)\boldsymbol{h}^H(\phi_k)\boldsymbol{R}_{zz}\boldsymbol{h}(\phi_k) + 0 \\
&= \frac{1}{N}\sigma^2\boldsymbol{g}^H(\phi_k)\boldsymbol{g}(\phi_k)\boldsymbol{h}^H(\phi_k)\boldsymbol{R}_{zz}\boldsymbol{h}(\phi_k) \\
&= \frac{1}{N}\sigma^2 H_{xkk}(\phi_k)\boldsymbol{h}^H(\phi_k)\bar{\boldsymbol{R}}_{zz}\boldsymbol{h}(\phi_k) \qquad \text{(B19)}
\end{aligned}
$$

$$
\begin{aligned}
&E\{\mu_{k1}\mu_{k2}^*\} \\
&= \frac{1}{N^2}E\Bigg\{\sum_{n=1}^{N}\sum_{t=1}^{N}\boldsymbol{g}^H(\phi_k)\boldsymbol{x}(n)\boldsymbol{z}^H(n)\boldsymbol{h}(\phi_k)\boldsymbol{g}^T(\phi_k)\boldsymbol{J}_M \\
&\qquad \cdot \boldsymbol{x}(t)\boldsymbol{z}^H(t)\bar{\boldsymbol{h}}^*(\phi_k)\Bigg\} \\
&= \frac{1}{N^2}\sum_{n=1}^{N}\sum_{t=1}^{N}\{E\{\boldsymbol{g}^H(\phi_k)\boldsymbol{x}(n)\boldsymbol{z}^H(n)\boldsymbol{h}(\phi_k)\} \\
&\qquad \cdot E\Big\{\boldsymbol{g}^T(\phi_k)\boldsymbol{J}_M\boldsymbol{x}(t)\boldsymbol{z}^H(t)\bar{\boldsymbol{h}}^*(\phi_k)\Big\} \\
&\qquad + E\{\boldsymbol{g}^H(\phi_k)\boldsymbol{x}(n)\boldsymbol{x}^T(t)\boldsymbol{J}_M\boldsymbol{g}(\phi_k)\} \\
&\qquad \cdot E\Big\{\bar{\boldsymbol{h}}^H(\phi_k)\boldsymbol{z}^*(t)\boldsymbol{z}^H(n)\boldsymbol{h}(\phi_k)\Big\} \\
&\qquad + E\Big\{\boldsymbol{g}^H(\phi_k)\boldsymbol{x}(n)\boldsymbol{z}^H(t)\bar{\boldsymbol{h}}^*(\phi_k)\Big\} \\
&\qquad \cdot E\{\boldsymbol{g}^T(\phi_k)\boldsymbol{J}_M\boldsymbol{x}(t)\boldsymbol{z}^H(n)\boldsymbol{h}(\phi_k)\}\} \\
&= \boldsymbol{g}^H(\phi_k)\boldsymbol{R}_{xz}\boldsymbol{h}(\phi_k)\boldsymbol{g}^T(\phi_k)\boldsymbol{J}_M\boldsymbol{R}_{xz}\bar{\boldsymbol{h}}^*(\phi_k) + 0 \\
&\quad + \frac{1}{N}\boldsymbol{g}^H(\phi_k)\bar{\boldsymbol{R}}_{xz}\bar{\boldsymbol{h}}^*(\phi_k)\boldsymbol{g}^T(\phi_k)\boldsymbol{J}_M\bar{\boldsymbol{R}}_{xz}\boldsymbol{h}(\phi_k) \\
&= 0 \qquad \text{(B20)}
\end{aligned}
$$

$$
\begin{aligned}
&E\{|\mu_{k2}|^2\} \\
&= \frac{1}{N^2}E\Bigg\{\sum_{n=1}^{N}\sum_{t=1}^{N}\boldsymbol{g}^H(\phi_k)\boldsymbol{J}_M\boldsymbol{x}^*(n)\boldsymbol{z}^T(n)\bar{\boldsymbol{h}}(\phi_k) \\
&\qquad \cdot \boldsymbol{g}^T(\phi_k)\boldsymbol{J}_M\boldsymbol{x}(t)\boldsymbol{z}^H(t)\bar{\boldsymbol{h}}^*(\phi_k)\Bigg\} \\
&= \frac{1}{N^2}\sum_{n=1}^{N}\sum_{t=1}^{N}\{E\{\boldsymbol{g}^H(\phi_k)\boldsymbol{J}_M\boldsymbol{x}^*(n)\boldsymbol{z}^T(n)\bar{\boldsymbol{h}}(\phi_k)\} \\
&\qquad \cdot E\Big\{\boldsymbol{g}^T(\phi_k)\boldsymbol{J}_M\boldsymbol{x}(t)\boldsymbol{z}^H(t)\bar{\boldsymbol{h}}^*(\phi_k)\Big\} \\
&\qquad + E\{\boldsymbol{g}^H(\phi_k)\boldsymbol{J}_M\boldsymbol{x}^*(n)\boldsymbol{x}^T(t)\boldsymbol{J}_M\boldsymbol{g}(\phi_k)\} \\
&\qquad \cdot E\Big\{\bar{\boldsymbol{h}}^T(\phi_k)\boldsymbol{z}(n)\boldsymbol{z}^H(t)\bar{\boldsymbol{h}}^*(\phi_k)\Big\} \\
&\qquad + E\Big\{\boldsymbol{g}^H(\phi_k)\boldsymbol{J}_M\boldsymbol{x}^*(n)\boldsymbol{z}^H(t)\bar{\boldsymbol{h}}^*(\phi_k)\Big\} \\
&\qquad \cdot E\Big\{\bar{\boldsymbol{h}}^T(\phi_k)\boldsymbol{z}(n)\boldsymbol{x}^T(t)\boldsymbol{J}_M\boldsymbol{g}(\phi_k)\Big\}\Big\} \\
&= \boldsymbol{g}^H(\phi_k)\bar{\boldsymbol{R}}_{xz}\bar{\boldsymbol{h}}(\phi_k)\boldsymbol{g}^T(\phi_k)\boldsymbol{J}_M\boldsymbol{R}_{xz}\bar{\boldsymbol{h}}^*(\phi_k) \\
&\quad + \frac{1}{N}\boldsymbol{g}^H(\phi_k)\boldsymbol{J}_M\boldsymbol{R}_{xx}^*\boldsymbol{J}_M\boldsymbol{g}(\phi_k)\bar{\boldsymbol{h}}^T(\phi_k)\boldsymbol{R}_{zz}\bar{\boldsymbol{h}}^*(\phi_k) + 0 \\
&= \frac{1}{N}\sigma^2 H_{xkk}\bar{\boldsymbol{h}}^T(\phi_k)\boldsymbol{R}_{zz}\bar{\boldsymbol{h}}^*(\phi_k). \qquad \text{(B21)}
\end{aligned}
$$

Therefore by substituting (B16)–(B21), (B14), and (B15) into (B8) and performing some straightforward manipulations, $\mathrm{MSE}(\hat{\phi}_k)$ of the estimated azimuth angle $\hat{\phi}_k$ in (30) can be readily obtained.

In the similar way, $\mathrm{MSE}(\hat{\theta}_k)$ of the estimated elevation angle $\hat{\theta}_k$ in (31) can be established immediately. ■

ACKNOWLEDGMENT

The authors would like to thank the anonymous reviewers and the Associate Editor Prof. S. Shahbazpanahi for their careful review and valuable comments and suggestions.

REFERENCES

[1] Y. Hua, T. K. Sarkar, and D. D. Weiner, "An L-shaped array for estimating 2-D directions of wave arrival," *IEEE Trans. Antennas Propag.*, vol. 39, no. 2, pp. 143–146, 1991.

[2] Y. Wu, G. Liao, and H. C. So, "A fast algorithm for 2-D direction-of-arrival estimation," *Signal Process.*, vol. 83, pp. 1827–1831, 2003.

[3] N. Tayem and H. M. Kwon, "L-shape 2-dimensional arrival angle estimation with propagator method," *IEEE Trans. Antennas Propag.*, vol. 53, no. 5, pp. 1622–1630, 2005.

[4] S. Kikuchi, H. Tsuji, and A. Sano, "Pair-matching method for estimating 2-D angle of arrival with a cross-correlation matrix," *IEEE Antennas Wireless Propag. Lett.*, vol. 5, pp. 35–40, 2006.

[5] J.-F. Gu and P. Wei, "Joint SVD of two cross-correlation matrices to achieve automatic pairing in 2-D angle estimation problems," *IEEE Antennas Wireless Propag. Lett.*, vol. 6, pp. 553–556, 2007.

[6] T. Xia, Y. Zheng, Q. Wan, and X. Wang, "Decoupled estimation of 2-D angles of arrival using two parallel uniform linear arrays," *IEEE Trans. Antennas Propag.*, vol. 55, no. 9, pp. 2627–2632, 2007.

[7] S. O. Al-Jazzar, D. C. McLernon, and M. A. Smadi, "SVD-based joint azimuth/elevation estimation with automatic pairing," *Signal Process.*, vol. 90, pp. 166–1675, 2010.

[8] T. Shu, X. Liu, and J. Lu, "Comments on 'L-shape 2-dimensional arrival angle estimation with propagator method'," *IEEE Trans. Antennas Propag.*, vol. 56, no. 5, pp. 1502–1503, 2008.

[9] S. Marcos, A. Marsal, and M. Benider, "The propagator method for sources bearing estimation," *Signal Process.*, vol. 42, pp. 121–138, 1995.

[10] J. Xin and A. Sano, "Computationally efficient subspace-based method for direction-of-arrival estimation without eigendecomposition," *IEEE Trans. Signal Process.*, vol. 52, no. 4, pp. 876–893, 2004.
[11] J. Xin, N. Zheng, and A. Sano, "Simple and efficient nonparametric method for estimating the number of signals without eigendecomposition," *IEEE Trans. Signal Process.*, vol. 55, no. 4, pp. 1405–1420, 2007.
[12] H. L. Van Trees, *Optimum Array Processing, Part IV of Detection, Estimation, and Modulation Theory*. New York: Wiley, 2002.
[13] A. J. van der Veen, P. B. Ober, and E. F. Deprettere, "Azimuth and elevation computation in high resolution DOA estimation," *IEEE Trans. Signal Process.*, vol. 40, no. 7, pp. 1828–1832, 1992.
[14] A. Swindlehurst and T. Kailath, "Azimuth/elevation direction finding using regular array geometries," *IEEE Trans. Aerosp. Electron. Syst.*, vol. 29, no. 1, pp. 145–156, 1993.
[15] C. P. Mathews and M. D. Zoltowski, "Eigenstructure techniques for 2-D angle estimation with uniform circular arrays," *IEEE Trans. Signal Process.*, vol. 42, no. 9, pp. 2395–2407, 1994.
[16] F. A. Sakarya and M. H. Hayes, "A subspace rotation-based technique for estimating 2-D arrival angles using nonlinear array configurations," *IEEE Trans. Signal Process.*, vol. 42, no. 2, pp. 409–411, 1994.
[17] P. Li, B. Yu, and J. Sun, "A new method for two-dimensional array signal processing in unknown noise environments," *Signal Process.*, vol. 47, pp. 319–327, 1995.
[18] M. D. Zoltowski, M. Haardt, and C. P. Mathews, "Closed-form 2-D angle estimation with rectangular arrays in element space or beamspace via unitary ESPRIT," *IEEE Trans. Signal Process.*, vol. 44, no. 2, pp. 316–328, 1996.
[19] C. P. Mathews, M. Haardt, and M. D. Zoltowski, "Performance analysis of closed-form ESPRIT based 2-D angle estimator for rectangular arrays," *IEEE Trans. Signal Process. Lett.*, vol. 3, no. 4, pp. 124–126, 1996.
[20] V. S. Kedia and B. Chandna, "A new algorithm for 2-D DOA estimation," *Signal Process.*, vol. 60, pp. 325–332, 1997.
[21] J. Ramos, C. P. Mathews, and M. D. Zoltowski, "FCA-ESPRIT: A closed-form 2-D angle estimation algorithm for filled circular arrays with arbitrary sampling lattices," *IEEE Trans. Signal Process.*, vol. 47, no. 1, pp. 213–217, 1997.
[22] N. Chotitakamthorn and J. A. Chambers, "IQML algorithm for multiple signal parameter estimation," *IEE Proc.-Radar, Sonar Navig.*, vol. 144, no. 5, pp. 237–244, 1997.
[23] J. E. Fernández del Río and M. F. Cátedra-Pérez, "The matrix pencil method for two-dimensional direction of arrival estimation employing an L-shaped array," *IEEE Trans. Antennas Propag.*, vol. 45, no. 11, pp. 1693–1697, 1997.
[24] T.-H. Liu and J. M. Mendel, "Azimuth and elevation direction finding using arbitrary array geometries," *IEEE Trans. Signal Process.*, vol. 46, no. 7, pp. 2061–2065, 1998.
[25] Y. Hua, "Estimating two-dimensional frequencies by matrix enhancement and matrix pencil," *IEEE Trans. Signal Process.*, vol. 40, no. 9, pp. 2267–2280, 1992.
[26] S. Rouquette and M. Najim, "Estimation of frequencies and damping factors by two-dimensional ESPRIT type methods," *IEEE Trans. Signal Process.*, vol. 49, no. 1, pp. 237–245, 2001.
[27] F.-J. Chen, C. C. Fung, C.-W. Kok, and S. Kwong, "Estimation of two-dimensional frequencies using modified matrix pencil method," *IEEE Trans. Signal Process.*, vol. 55, no. 2, pp. 718–724, 2007.
[28] Q. Y. Yin, R. W. Newcomb, and L. H. Zou, "Estimating 2-D angles of arrival via two parallel linear arrays," in *Proc. IEEE Int. Conf. Acoust., Speech, Signal Process.*, Glasgow, Scotland, May 1989, pp. 2803–2806.
[29] Z. Ye, Y. Zhang, and X. Xu, "Two-dimensional direction of arrival estimation in the presence of uncorrelated and coherent signals," *IET Signal Process.*, vol. 3, no. 5, pp. 416–429, 2009.
[30] J. He and Z. Liu, "Extended aperture 2-D direction finding with a two-parallel-shaped-array using propagator method," *IEEE Antennas Wireless Propag. Lett.*, vol. 8, pp. 323–327, 2009.
[31] J. Liang and D. Liu, "Joint elevation and azimuth direction finding using L-shaped array," *IEEE Trans. Antennas Propag.*, vol. 58, no. 6, pp. 2136–2141, 2010.
[32] R. Roy and T. Kalaith, "ESPRIT—Estimation of signal parameters via rational invariance techniques," *IEEE Trans. Acoust., Speech, Signal Process.*, vol. 37, no. 7, pp. 984–995, 1989.
[33] M. Haardt and J. A. Nossek, "Unitary ESPRIT: How to obtain increased estimation accuracy with a reduced computational burden," *IEEE Trans. Signal Process.*, vol. 43, no. 5, pp. 1232–1242, 1995.
[34] F. Gao and A. B. Gershman, "A generalized ESPRIT approach to direction-of-arrival estimation," *IEEE Trans. Signal Process. Lett.*, vol. 12, no. 3, pp. 254–257, 2005.
[35] L. Gan, J.-F. Gu, and P. Wei, "Estimation of 2-D DOA for noncircular sources using simultaneous SVD technique," *IEEE Antennas Wireless Propag. Lett.*, vol. 7, pp. 385–388, 2008.
[36] N.-J. Li, J.-F. Gu, and P. Wei, "2-D DOA estimation via matrix partition and stacking technique," *EURASIP J. Adv. in Signal Process.*, vol. 2009, pp. 1–8, 2009, Article ID: 896284.
[37] P. Comon and G. H. Golub, "Tracking a few extreme singular values and vectors in signal processing," *Proc. IEEE*, vol. 78, no. 8, pp. 1327–1343, 1990.
[38] P. H. M. Janssen and P. Stoica, "On the expectation of the product of four matrix-valued Gaussian random variables," *IEEE Trans. Autom. Control*, vol. 33, no. 9, pp. 867–870, 1988.
[39] P. Stoica and A. Nehorai, "Performance study of conditional and unconditional direction-of-arrival estimation," *IEEE Trans. Acoust., Speech, Signal Process.*, vol. 38, no. 10, pp. 1783–1795, 1990.
[40] J. Xin, N. Zheng, and A. Sano, "Subspace-based adaptive method for estimating direction-of-arrival with Luenberger observer," *IEEE Trans. Signal Process.*, vol. 59, no. 1, pp. 145–159, 2011.
[41] L. Ljung, "Analysis of recursive stochastic algorithms," *IEEE Trans. Autom. Control*, vol. 22, no. 4, pp. 551–575, 1977.
[42] C. G. Samson and V. U. Reddy, "Fixed point error analysis of the normalized ladder algorithm," *IEEE Trans. Acoust., Speech, Signal Process.*, vol. 31, no. 5, pp. 1177–1191, 1983.
[43] R. O. Schmidt, "Multiple emitter location and signal parameter estimation," in *Proc. RADC Spectrum Estimation Workshop*, Rome, NY, Oct. 1979, pp. 243–258.
[44] A. J. Barabell, "Improving the resolution performance of eigenstructure-based direction-finding algorithms," in *Proc. IEEE Int. Conf. Acoust., Speech, Signal Process.*, Boston, MA, 1983, vol. 1, pp. 336–339.
[45] P. Stoica and K. C. Sharman, "Maximum likelihood methods for direction-of-arrival estimation," *IEEE Trans. Acoust., Speech, Signal Process.*, vol. 38, no. 7, pp. 1132–1143, 1990.
[46] P. Stoica and T. Söderström, "Statistical analysis of a subspace method for bearing estimation without eigendecomposition," *IEE Proc.*, vol. 139, no. 4, pt. F, pp. 301–305, 1992.
[47] R. O. Schmidt, "Multiple emitter location and signal parameter estimation," *IEEE Trans. Antennas Propag.*, vol. 34, no. 3, pp. 276–280, 1986.

Guangmin Wang (S'11) received the B.E. degree in information and communication engineering from Xi'an Jiaotong University, Xi'an, China, in 2008.

He is currently working toward the Ph.D. degree with the Department of Control Science and Engineering, Xi'an Jiaotong University, Xi'an, China. His current research interests include array and statistical signal processing.

Jingmin Xin (S'92–M'96–SM'06) received the B.E. degree in information and control engineering from Xi'an Jiaotong University, Xi'an, China, in 1988, and the M.S. and Ph.D. degrees in electrical engineering from Keio University, Yokohama, Japan, in 1993 and 1996, respectively.

From 1988 to 1990, he was with the Tenth Institute of Ministry of Posts and Telecommunications (MPT) of China, Xi'an. He was with the Communications Research Laboratory, Japan, as an Invited Research Fellow of the Telecommunications Advancement Organization of Japan (TAO) from 1996 to 1997 and as a Postdoctoral Fellow of the Japan Science and Technology Corporation (JST) from 1997 to 1999. He was also a Guest (Senior) Researcher with YRP Mobile Telecommunications Key Technology Research Laboratories Company, Limited, Yokosuka, Japan, from 1999 to 2001. From 2002 to 2007, he was with Fujitsu Laboratories Limited, Yokosuka, Japan. Since 2007, he has been a Professor at Xi'an Jiaotong University. His research interests are in the areas of adaptive filtering, statistical and array signal processing, system identification, and pattern recognition.

Nanning Zheng (SM'93–F'06) graduated from the Department of Electrical Engineering, Xi'an Jiaotong University, Xi'and, China, in 1975, and received the M.S. degree in information and control engineering from Xi'an Jiaotong University in 1981 and the Ph.D. degree in electrical engineering from Keio University, Yokohama, Japan, in 1985.

He joined Xi'an Jiaotong University in 1975, and is currently a Professor and the Director of the Institute of Artificial Intelligence and Robotics, Xi'an Jiaotong University. His research interests include computer vision, pattern recognition and image processing, and hardware implementation of intelligent systems.

Dr. Zheng became a member of the Chinese Academy of Engineering in 1999, and he is the Chinese Representative on the Governing Board of the International Association for Pattern Recognition. He also serves as an executive deputy editor of the *Chinese Science Bulletin*.

Akira Sano (M'89) received the B.E., M.S., and Ph.D. degrees in mathematical engineering and information physics from the University of Tokyo, Japan, in 1966, 1968, and 1971, respectively.

In 1971, he joined the Department of Electrical Engineering, Keio University, Yokohama, Japan, where he was a Professor with the Department of System Design Engineering till 2009, and he is currently Professor Emeritus of Keio University. He is a member of Science Council of Japan since 2005. He was a Visiting Research Fellow at the University of Salford, Salford, U.K., from 1977 to 1978. His current research interests are in adaptive modeling and design theory in control, signal processing and communication, and applications to control of sounds and vibrations, mechanical systems, and mobile communication systems. He is a coauthor of the textbook *State Variable Methods in Automatic Control* (New York: Wiley, 1988).

Dr. Sano received the Kelvin Premium from the Institute of Electrical Engineering in 1986. He is a Fellow of the Society of Instrument and Control Engineers and is a Member of the Institute of Electrical Engineering of Japan and the Institute of Electronics, Information and Communications Engineers of Japan. He was General Co-Chair of 1999 IEEE Conference of Control Applications and an IPC Chair of 2004 IFAC Workshop on Adaptation and Learning in Control and Signal Processing. He served as Chair of IFAC Technical Committee on Modeling and Control of Environmental Systems from 1996 to 2001. He has also been Vice Chair of IFAC Technical Committee on Adaptive Control and Learning since 1999 and has been Chair of IFAC Technical Committee on Adaptive and Learning Systems since 2002. He was also on the Editorial Board of *Signal Processing*.